Unitary Differential Space-Time-Frequency Codes for MB-OFDM UWB Wireless Communications

L. C. Tran, *Member, IEEE*, A. Mertins, *Senior Member, IEEE*,
and T. A. Wysocki, *Senior Member, IEEE*

***Abstract*—In a multiple-input multiple-output (MIMO), multi-band orthogonal frequency division multiplexing (MB-OFDM) ultra-wideband (UWB) system, coherent detection requires the transmission of a large number of symbols for channel estimation, thus reducing the bandwidth efficiency. For the first time, this paper proposes unitary differential space-time-frequency codes (DSTFCs) for MB-OFDM UWB communications, which increase the system bandwidth efficiency because no channel state information (CSI) is required. The proposed system would be useful when CSI is unavailable at the receiver, such as when the transmission of multiple channel estimation symbols is impractical or uneconomical. The coding and decoding algorithms for the proposed DSTFCs are then derived for both constant envelope modulation scheme, such as PSK (phase shift keying) and 4QAM (quadrature amplitude modulation), and multi-dimensional modulation scheme, such as DCM (dual carrier modulation). The paper also quantifies for the first time the diversity order of a DSTFC MB-OFDM system. Simulation results show that the application of DSTFCs can significantly improve the bit error performance of conventional differential MB-OFDM system (without MIMO), and even provide much better bit error performance than the conventional coherent MB-OFDM system (without MIMO) at high signal-to-noise ratios.**

***Index Terms*—UWB, MB-OFDM, DSTFC, STFC, MIMO.**

I. Introduction

COMBINATION of the emerging technologies, namely multi-band orthogonal frequency division multiplexing ultra-wideband (MB-OFDM UWB) [3], [4], multiple-input multiple-output (MIMO), and space-time-frequency codes (STFCs), may provide a significant improvement in the form of maximum achievable communication range, bit error performance, system capacity, data rate, or a combined form of those. The combination of MB-OFDM UWB, MIMO and STFCs to which we will refer as STFC MB-OFDM UWB systems has been considerably examined in the literature, such as [5], [6], [7], [8], [9], [10], [11].

In all aforementioned works, channel state information (CSI) is assumed to be known exactly at the receiver, allowing the receiver to perform coherent detection. According to [3], six MB-OFDM symbols are transmitted in the physical layer convergence protocol (PLCP) preamble for channel estimation between each pair of transmit (Tx) and receive (Rx) antennas, thus facilitating coherent detection at the receiver. In a MIMO system consisting of M Tx and N Rx antennas, the required number of symbols for this purpose might be as large as $6M$, unless when superimposed training techniques, such as the ones mentioned in [12], [13], [14], are used to reduce the number of channel estimation symbols transmitted within the preamble. Therefore, transmission of a large number of MB-OFDM symbols for channel estimation reduces significantly the system bandwidth efficiency. Moreover, in fast fading channels or in very high data rate systems, transmission of a large number of MB-OFDM symbols for channel estimation is a hassling task and might even be impractical or uneconomical. In these cases, non-coherent detection (or differential detection), where no CSI is required for decoding signals at the receiver, would be the best candidate.

For differential transmission in general OFDM systems associated with a MIMO model, various techniques have been proposed in the literature, such as [15], [16], [17], [18], [19] and [20]. However, differential transmission in MB-OFDM systems associated with MIMO has not been considered yet. There are two main differences between channel characteristics in conventional OFDM systems and in MB-OFDM UWB ones. First, channels in the latter are much more dispersive than those in the former, with the average number of multipaths possibly reaching some thousands [21]. Second, channel coefficients in the former are usually considered to be Rayleigh distributed, while those in the latter are log-normally distributed [21]. Therefore, the systems incorporating MB-OFDM UWB, MIMO and differential transmission must be more specifically analyzed, though there exist several similarities between those systems and the systems incorporating conventional OFDM, MIMO and differential transmission.

Thus this paper is the first case study to examine the application of differential space-time-frequency codes (DSTFCs) in MB-OFDM UWB communications. Contributions of this paper include the implementation framework of DSTFCs, which are adapted from the STFCs that we proposed previously in [7] to apply to a differential detection scenario, in a MB-OFDM UWB system; the derivation of in-depth differential coding and decoding algorithms in the case of constant envelop modulation schemes, such as M-PSK and 4-QAM; the novel coding and decoding algorithms for the case of

Manuscript received March 25, 2012; revised August 9 and November 4, 2012; accepted November 6, 2012. The associate editor coordinating the review of this paper and approving it for publication was A. Giorgetti.

The material of this paper has been partially published in [1] and [2].

L. C. Tran is with the School of Electrical, Computer and Telecommunications Engineering, University of Wollongong, Australia (e-mail: lctran@uow.edu.au).

A. Mertins is with the Institute for Signal Processing, University of Lübeck, Lübeck, Germany (e-mail: mertins@isip.uni-luebeck.de).

T. A. Wysocki is with the Peter Kiewit Institute, University of Nebraska-Lincoln, USA (e-mail: twysocki2@unl.edu).

Digital Object Identifier 10.1109/TWC.2012.122212.120436

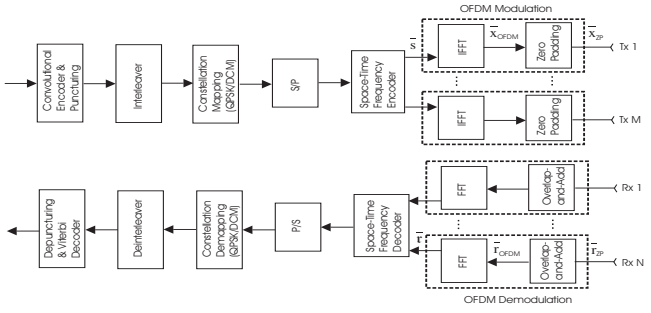

Fig. 1. STFC MB-OFDM UWB system [7].

multi-dimensional modulation schemes, such as Dual Carrier Modulation; the mathematical evaluation of the diversity order of the proposed DSTFC MB-OFDM system, and the in-depth simulation results.

The paper is organized as follows. Section II reviews briefly the mathematical model of our proposed STFC MB-OFDM UWB system [7]. In Section III, unitary DSTFCs are proposed for MB-OFDM UWB, and decoding metrics are derived for the proposed DSTFCs in Section IV. Section V formulates the pairwise error probability and the maximum achievable diversity order of the proposed DSTFC MB-OFDM system. Simulation results are mentioned in Section VI and conclusions are drawn in Section VII.

Notations: Throughout the paper, the superscripts $(.)^*$, $(.)^T$ and $(.)^H$ denote the complex conjugation, transposition and conjugate transpose operation, respectively. We denote $\bar{\mathbf{a}}_j \bullet \bar{\mathbf{b}}_j$, $\bar{\mathbf{a}}_j * \bar{\mathbf{b}}_j$ and $\bar{\mathbf{a}}_j \otimes \bar{\mathbf{b}}_j$ to be the element-wise (or Hadamard) product, the linear convolution operation, and the cyclic convolution operation between the two vectors $\bar{\mathbf{a}}_j$ and $\bar{\mathbf{b}}_j$, respectively. Further, $\bar{\mathbf{a}}.\hat{}\,2$ denotes the element-wise power-2 operation of $\bar{\mathbf{a}}$. We define the multiplication operation $\mathbf{C} \circ \mathbf{D}$ between the two matrices $\mathbf{C} = \{\bar{\mathbf{c}}_{t,m}\}_{T\times M}$ and $\mathbf{D} = \{\bar{\mathbf{d}}_{m,n}\}_{M\times N}$, whose elements $\bar{\mathbf{c}}_{t,m}$ and $\bar{\mathbf{d}}_{m,n}$ are column vectors of the same length, such that the (t,n)-th element of the resulting matrix is a column vector $\sum_{m=1}^{M} \bar{\mathbf{c}}_{t,m} \bullet \bar{\mathbf{d}}_{m,n}$. Denote N_{fft} to be the FFT/IFFT size (for MB-OFDM UWB communications [3], $N_{\text{fft}} = 128$). Further, $\Re\{c\}$ and $\Im\{c\}$ denote the real and imaginary parts of the complex number c. The notation $\text{diag}(\bar{\mathbf{a}}_j)$ denotes a square diagonal matrix formed by stacking the vector $\bar{\mathbf{a}}_j$ on the main diagonal of the matrix, while $\{\text{diag}(\bar{\mathbf{a}}_j)\}_{M_j\times N_j}$ denotes a $M_j \times N_j$-sized rectangular matrix whose elements are diagonal matrices $\text{diag}(\bar{\mathbf{a}}_j)$. We state that the two subsets of indices $\{m,k\}$ and $\{\acute{m},\acute{k}\}$ to be different, denoted as $\{m,k\} \neq \{\acute{m},\acute{k}\}$, if at least one of the following two inequalities $m \neq \acute{m}$ and $k \neq \acute{k}$ occurs. Finally, we define $\bar{\mathbf{1}}$ as a column vector of length N_D, whose elements are all ones.

II. STFC MB-OFDM UWB System

The proposed STFC MB-OFDM UWB system [7] consisting of M Tx antennas and N Rx antennas, with the notations of signals at the considered reference points, is depicted in Fig. 1. The transmitted STFC is denoted as a matrix $\mathbf{S}_t = \{\bar{\mathbf{s}}_{t,m}\}_{T\times M}$, where T is the number of MB-OFDM symbol time slots required to transmit the whole STFC block. Each MB-OFDM symbol time slot is $T_{SYM} = 312.5$ ns, including the FFT/IFFT period $T_{FFT} = 242.42$ ns and the zero padded suffix duration of $T_{ZPS} = 70.08$ ns [3, Table 6-2], [4, Table 6-2]. The code matrix $\mathbf{S}$ can be structured in a similar way as orthogonal space-time block codes (OSTBCs) [22], [23], [24] or quasi-orthogonal space-time block codes (QOSTBCs) [25] in conventional wireless STBC MIMO systems, except that each element $\bar{\mathbf{s}}_{t,m}$ is not a complex number, but is defined as a column vector $\bar{\mathbf{s}}_{t,m} = [s_{t,m,1}\ s_{t,m,2} \dots s_{t,m,N_{\text{fft}}}]^T$. The vectors $\bar{\mathbf{s}}_{t,m}$ comprises the original transmitted data before IFFT. The symbols $s_{t,m,k}$, for $k = 1,\dots,N_{\text{fft}}$, are drawn from a PSK (phase shift keying), QAM (quadrature amplitude modulation), DCM (dual carrier modulation) [26], or MDCM (modified dual carrier modulation) [4] signal constellation.

Denote $\mathcal{X} = \{\bar{\mathbf{x}}_{\text{OFDM},t,m}\}_{T\times M}$ to be the matrix whose elements are the N_{fft}-point IFFTs of the respective elements in $\mathbf{S}_t$, then $\mathcal{X} = \{\text{IFFT}\{\bar{\mathbf{s}}_{t,m}\}\}_{T\times M} = \{\bar{\mathbf{x}}_{\text{OFDM},t,m}\}_{T\times M}$. The symbols $\bar{\mathbf{x}}_{\text{OFDM},t,m}$ are referred to as MB-OFDM symbols. Further, denote $\mathcal{X}_{\mathbf{ZP}} = \{\bar{\mathbf{x}}_{ZP,t,m}\}_{T\times M}$ to be the matrix whose elements are the respective elements in $\mathcal{X}$ appended by a zero padded suffix (ZPS) of 37 zeros [3]. At the transmission of the t-th MB-OFDM symbol, we denote $\bar{\mathbf{h}}_{t,m,n} = [h_{t,m,n,1}\ h_{t,m,n,2} \dots h_{t,m,n,L_{m,n}}]^T$ to be the channel vector between the m-th Tx and n-th Rx antennas, for $m = 1,\dots,M, n = 1,\dots,N$, where the channel coefficients $h_{t,m,n,l}$ of the l-th path, $l = 1,\dots,L_{m,n}$, in this channel are modeled as independently *log-normally* distributed random variables (RVs) [21]. Let $L_{max} = \max\{L_{m,n}\}$, for $m = 1,\dots,M, n = 1,\dots,N$. Denote the MB-OFDM UWB channel coefficient matrix as $\mathbf{H}_t = \{\bar{\mathbf{h}}_{t,m,n,ZP}\}_{M\times N}$ where the vector $\bar{\mathbf{h}}_{t,m,n,ZP}$ is created from the corresponding channel vector $\bar{\mathbf{h}}_{t,m,n}$ by adding zeros to have the length L_{max}.

At the transmission of the t-th MB-OFDM symbol, the received signal at the n-th Rx antenna is calculated as

$$\bar{\mathbf{r}}_{ZP,t,n} = \sum_{m=1}^{M} \left(\bar{\mathbf{x}}_{ZP,t,m} * \bar{\mathbf{h}}_{t,m,n}\right) + \bar{\mathbf{n}}_{t,n}. \quad (1)$$

The elements of noise vector $\bar{\mathbf{n}}_{t,n}$ are considered to be independent complex Gaussian RVs.

In MB-OFDM systems, a ZPS of length $N_{ZPS} = 37$ [3] is appended to each symbol $\bar{\mathbf{x}}_{\text{OFDM},t,m}$ at the transmitter to create a transmitted symbol $\bar{\mathbf{x}}_{ZP,t,m}$. At the receiver, an overlap-and-add operation (OAAO) must be performed before FFT. This means that N_{ZPS} samples of a received symbol $\bar{\mathbf{r}}_{ZP,t,n}$, from $(N_{\text{fft}}+1)$ to $(N_{\text{fft}}+N_{ZPS})$, are added to the beginning of that received symbol. Then the first N_{fft} samples of the resulting symbol will be used to decode the transmitted symbol. As a result, after performing OAAO for the received signal $\bar{\mathbf{r}}_{ZP,t,n}$ in (1) and then taking the first N_{fft} resulting samples, denoted as $\bar{\mathbf{r}}_{\text{OFDM},t,n}$, the following equation is deduced

$$\bar{\mathbf{r}}_{\text{OFDM},t,n} = \sum_{m=1}^{M} \bar{\mathbf{x}}_{\text{OFDM},t,m} \otimes \bar{\mathbf{h}}_{t,m,n} + \bar{\mathbf{n}}_{t,n}. \quad (2)$$

TABLE I
NUMBERS OF MULTIPATHS Np_{10dB}, $Np_{85\%}$, AND $\bar{N}_p$ [21].

	CM1	CM2	CM3	CM4
Np_{10dB}	12.5	15.3	24.9	41.2
$Np_{85\%}$	20.8	33.9	64.7	123.3
$\bar{N}_p$	287.9	739.5	1463.7	3905.5

For the circular convolution, we have the following property

$$\begin{aligned}\bar{\mathbf{x}}_{\mathrm{OFDM},t,m} \otimes \bar{\mathbf{h}}_{t,m,n} &= \mathrm{IFFT}\{\mathrm{FFT}\{\bar{\mathbf{x}}_{\mathrm{OFDM},t,m}\} \bullet \mathrm{FFT}\{\bar{\mathbf{h}}_{t,m,n}\}\} \\ &= \mathrm{IFFT}\{\bar{\mathbf{s}}_{t,m} \bullet \bar{\mathfrak{h}}_{t,m,n}\}, \end{aligned} \quad (3)$$

where $\bar{\mathfrak{h}}_{t,m,n}$ is the N_{fft}-point FFT of the channel vector $\bar{\mathbf{h}}_{t,m,n}$, i.e. $\bar{\mathfrak{h}}_{t,m,n} = \mathrm{FFT}\{\bar{\mathbf{h}}_{t,m,n}\}$. We denote $\bar{\mathfrak{h}}_{t,m,n} = [\hbar_{t,m,n,1}\ \hbar_{t,m,n,2} \dots \hbar_{t,m,n,N_{\mathrm{fft}}}]^T$.

It is noted that the exact transition from (1) to (2) can only be achieved if the length of ZPS is not smaller than the number of the channel multipaths. In fact, the length of ZPS in a MB-OFDM UWB system $N_{ZPS} = 37$ is much smaller than the average number of multipaths $\bar{N}_p$ of UWB channels, which may reach some thousands (cf. Table I). Therefore, this transition cannot be an exact equality, but an approximation. This will be discussed further in Section V-C of this paper.

From (2) and (3), after the FFT operation at the receiver, the received signal becomes

$$\mathrm{FFT}\{\bar{\mathbf{r}}_{\mathrm{OFDM},t,n}\} = \sum_{m=1}^{M} \bar{\mathbf{s}}_{t,m} \bullet \bar{\mathfrak{h}}_{t,m,n} + \mathrm{FFT}\{\bar{\mathbf{n}}_{t,n}\}. \quad (4)$$

Denote $\bar{\mathfrak{r}}_{t,n} = [\mathfrak{r}_{t,n,1}\ \mathfrak{r}_{t,n,2} \dots \mathfrak{r}_{t,n,N_{\mathrm{fft}}}]^T = \mathrm{FFT}\{\bar{\mathbf{r}}_{\mathrm{OFDM},t,n}\}$ and $\bar{\mathfrak{n}}_{t,n} = [\mathfrak{n}_{t,n,1}\ \mathfrak{n}_{t,n,2} \dots \mathfrak{n}_{t,n,N_{\mathrm{fft}}}]^T = \mathrm{FFT}\{\bar{\mathbf{n}}_{t,n}\}$. Then (4) can be rewritten as follows

$$\bar{\mathfrak{r}}_{t,n} = \sum_{m=1}^{M} \bar{\mathbf{s}}_{t,m} \bullet \bar{\mathfrak{h}}_{t,m,n} + \bar{\mathfrak{n}}_{t,n}. \quad (5)$$

Recall that $\bar{\mathbf{s}}_{t,m}$ is the original modulated signal (before IFFT).

Denote $\mathcal{H}_\mathbf{t} = \{\bar{\mathfrak{h}}_{t,m,n}\}_{M\times N}$ to be the matrix whose elements are the N_{fft}-point FFTs of the respective elements in the channel coefficient matrix $\mathbf{H}_t$, and $\mathcal{N} = \{\bar{\mathfrak{n}}_{t,n}\}_{T\times N}$ to be the noise matrix. We can rewrite (5) in matrix form as follows

$$\mathcal{R}_\mathbf{t} = \mathbf{S}_t \circ \mathcal{H}_\mathbf{t} + \mathcal{N}_\mathbf{t}. \quad (6)$$

If we rewrite $\mathcal{R}_\mathbf{t}$, $\mathbf{S}_t$, $\mathcal{H}_t$ and $\mathcal{N}_t$ in (6) in the following forms

$$\begin{aligned}\mathbb{R}_t &= \{\mathrm{diag}(\bar{\mathfrak{r}}_{t,n})\}_{TN_{\mathrm{fft}}\times NN_{\mathrm{fft}}}, \\ \mathbb{H}_t &= \{\mathrm{diag}(\bar{\mathfrak{h}}_{t,m,n})\}_{MN_{\mathrm{fft}}\times NN_{\mathrm{fft}}}, \\ \mathbb{S}_t &= \{\mathrm{diag}(\bar{\mathbf{s}}_{t,m})\}_{TN_{\mathrm{fft}}\times MN_{\mathrm{fft}}}, \\ \mathbb{N}_t &= \{\mathrm{diag}(\bar{\mathfrak{n}}_{t,n})\}_{TN_{\mathrm{fft}}\times NN_{\mathrm{fft}}}, \end{aligned} \quad (7)$$

then (6) can be rewritten with the normal definition of matrix multiplication as follows

$$\mathbb{R}_t = \mathbb{S}_t\mathbb{H}_t + \mathbb{N}_t.$$

For coherent detection, channel coefficients are assumed to be known at the receiver. In this case, if $\mathbf{S}_t$ is a full orthogonal STFC, each MB-OFDM symbol $\bar{\mathbf{s}}_{t,m}$, which is a $(N_{\mathrm{fft}} \times 1)$-sized column vector, can be decoded separately [7]. The decoding process can even be more simplified by the fact that each element $s_{t,m,j}$ within $\bar{\mathbf{s}}_{t,m}$ can also be decoded separately. If $\mathbf{S}_t$ is partially orthogonal, i.e. $\mathbf{S}_t$ is a quasi-orthogonal STFC (QOSTFC) [10], [11], each pair of MB-OFDM symbols each of which is a $(N_{\mathrm{fft}} \times 1)$-sized column vector can be decoded separately. Similarly, the decoding process can be more simplified by the fact that each pair of elements within the pair of MB-OFDM symbols can also be decoded separately. We refer readers to our publications [7], [10], [11] for more detail about the decoding metrics of STFCs and QOSTFCs in the case of coherent detection.

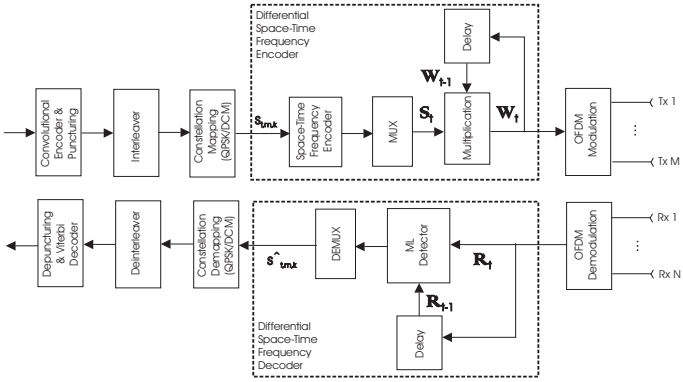

Fig. 2. Structural diagram of the proposed DSTFC MB-OFDM UWB system.

III. DSTFCs FOR MB-OFDM UWB COMMUNICATIONS

The proposed model of a DSTFC MB-OFDM UWB system requiring no transmission of channel estimation symbols is depicted in Fig. 2. In this figure, we refer the two novel blocks to as the multiplexing (MUX) and demultiplexing (DEMUX) blocks. These two blocks are transparent, i.e. having no effect to the system, if constant envelop modulation schemes (e.g. PSK and 4QAM) are used, but non-transparent in the case of DCM scheme. The exact functions of the MUX and DEMUX blocks will be mentioned in Section IV-B of this paper.

We consider the application of the Alamouti STFC

$$\mathbf{S}_\mathbf{t} = 1/\sqrt{2}\begin{bmatrix} \bar{\mathbf{s}}_{t,1} & \bar{\mathbf{s}}_{t,2} \\ -\bar{\mathbf{s}}_{t,2}^* & \bar{\mathbf{s}}_{t,1}^* \end{bmatrix}, \quad (8)$$

where the MB-OFDM symbol $\bar{\mathbf{s}}_{t,m}$, for $m = 1, 2$, is a column vector of N_{fft} complex symbols corresponding to N_{fft} sub-carriers, i.e. $\bar{\mathbf{s}}_{t,m} = [s_{t,m,1}\ \ s_{t,m,2} \dots s_{t,m,N_{\mathrm{fft}}}]^T$. Channels in the DSTFC MB-OFDM system are assumed to be constant during a time window of K consecutive transmitted DSTFC code blocks, i.e. during $2KT_{SYM}$ (ns), where K is an integer number and T_{SYM} is the MB-OFDM symbol interval $T_{SYM} = 312.5$ ns [3]. Similarly to Eq. (7), the STFC in (8) can be rewritten in the following form

$$\mathbb{S}_t = 1/\sqrt{2}\begin{bmatrix} \mathrm{diag}(\bar{\mathbf{s}}_{t,1}) & \mathrm{diag}(\bar{\mathbf{s}}_{t,2}) \\ -\mathrm{diag}(\bar{\mathbf{s}}_{t,2}^*) & \mathrm{diag}(\bar{\mathbf{s}}_{t,1}^*) \end{bmatrix}. \quad (9)$$

The proposed DSTFC MB-OFDM system initializes the transmission with an identity matrix $\mathbb{W}_0 = I_{2N_{\mathrm{fft}}}$. The

subsequent code matrices will be generated and transmitted according to the following principle

$$\mathbb{W}_t \quad = \quad \mathbb{S}_t \mathbb{W}_{t-1}. \tag{10}$$

The transmission model can be expressed as follows

$$\mathbb{R}_t \quad = \quad \mathbb{W}_t \mathbb{H}_t + \mathbb{N}_t. \tag{11}$$

Since channels are assumed to be constant during the transmission of K consecutive Alamouti STFC blocks, i.e. within a time window $2KT_{SYM}$ (ns), the encoding principle (10) should be applied for $t = 1, \ldots, (K-1)$ and the whole transmission protocol is reset for a new time window.

As mentioned detailed in Section IV, the proposed DSTFC MB-OFDM concept would work well if the channel coefficients are assumed to be constant during *at least* two consecutive DSTFC blocks (i.e. $K \geq 2$). This assumption is in fact normally the case. In practice, the UWB channel is typically unchanged during several tens of Alamouti DSTFC blocks to several thousands of DSTFC blocks. Therefore, the case where the channel changes after every two consecutive Alamouti DSTFC blocks is merely the fastest fading case where the proposed DSTFC concept still works accurately. If the channel matrix changes in every block, the difference of channels during different code blocks results in interference in the differential decoding process, thus the system performance would be degraded.

Let us consider the following two scenarios, illustrating when coherent and differential STFC MB-OFDM systems should be deployed.

Example 1: We consider the scenario where the Alamouti STFC is deployed for a wireless personal area network (WPAN) with the carrier frequency $F_c = 3.432$ GHz, speed of the mobile terminal $v = 5$ km/h (walking speed), i.e. $v = 1.39$ m/s. It is known that the MB-OFDM symbol period is $T_{SYM} = 312.5$ ns (including $T_{FFT} = 242.42$ ns and $T_{ZPS} = 70.08$ ns). The maximum Doppler frequency is calculated as [27]

$$f_m = \frac{vF_c}{c} = \frac{1.39 \times 3.432 \times 10^9}{3 \times 10^8} = 15.89 \ Hz.$$

The average coherence time T_C of the channel is estimated by the following empirical formula [27]

$$T_C \quad = \quad \frac{0.423}{f_m} = \frac{0.423}{15.89} = 26.62 \ ms.$$

This means that the channel can be considered to be constant during $T_C/T_{SYM} = 85,184$ MB-OFDM symbols. In other words, the channel is almost unchanged during 42,592 consecutive Alamouti STFC blocks. Clearly, STFC MB-OFDM communications with coherent detection should be used in this case, since the channel coherence time is large enough to allow the transmission of a large signal overhead for the channel estimation purpose.

Example 2: We consider another scenario where the Alamouti STFC is deployed in a magnetic bearing system with the carrier frequency $F_c = 10.296$ GHz. The transmitter is located at the center, while the receiver is placed on a rotor, rotating around the transmitter. According to SKF Magnetic Bearings - a world leader in design, development, manufacture and implementation of magnetic bearings - a magnetic bearing may allow the surface speed up to or exceed 250 m/s (i.e. 4.5 million DNs where the unit DN is the rotor diameter in millimeters times the angular speed in rounds per minute) [28]. Hence, the maximum Doppler frequency is

$$f_m = \frac{vF_c}{c} = \frac{250 \times 10.296 \times 10^9}{3 \times 10^8} = 8,580 \ Hz.$$

This results in the average channel coherence time

$$T_C \quad = \quad \frac{0.423}{f_m} = \frac{0.423}{8,580} = 49.3 \ \mu s.$$

The channel now can be considered to be constant during approximately $T_C/T_{SYM} \approx 158$ MB-OFDM symbols, i.e. 79 consecutive Alamouti STFC blocks. Clearly, the channel coherence time shortens significantly, compared to the previous scenario. This example might suggest that the differential transmission could be more economical for a MIMO MB-OFDM UWB system, since it does not require a large signal overhead for the channel estimation purpose, which can be as large as $6M$ symbols, where M denotes the number of Tx antennas. The proposed DSTFC concept is one of the excellent candidates for this scenario.

IV. Maximum Likelihood Decoding for DSTFC MB-OFDM

A. Constant Envelope Modulation Schemes

We first derive the maximum likelihood (ML) decoding metric for the proposed DSTFC in the case of signal constellations with constant envelopes, such as PSK and 4QAM, and with one Rx antenna. For simplicity, the index of the Rx antenna is omitted.

The STFC in (9) could be represented in the following form

$$\mathbb{S}_t = \frac{1}{\sqrt{2}} \sum_{m=1}^{2} \sum_{k=1}^{N_{\text{fft}}} (\mathbb{X}_{t,m,k} s^R_{t,m,k} + i \mathbb{Y}_{t,m,k} s^I_{t,m,k}), \tag{12}$$

where $s^R_{t,m,k}$ and $s^I_{t,m,k}$ are the real and imaginary parts of the symbol $s_{t,m,k}$ respectively, i.e. $s_{t,m,k} = s^R_{t,m,k} + i s^I_{t,m,k}$, while $\mathbb{X}_{t,m,k}$ and $\mathbb{Y}_{t,m,k}$ are their corresponding weighting matrices. It is easy to realize that the weighting matrices are real, square, orthogonal matrices. We assume that the normalized power of each symbol $s_{t,m,k}$ within $\bar{\mathbb{s}}_{t,m}$, for $k = 1, \ldots, N_{\text{fft}}$, is unitary, i.e. $|s_{t,m,k}|^2 = 1$. Hence $s_{t,m,k}$ can be drawn from a unitary PSK or 4QAM signal constellation that is denoted as $\mathcal{C}$. As a result, $\mathbb{S}_t$ and $\mathbb{W}_t$, which is constructed based on (10), are unitary matrices of size $2N_{\text{fft}}$, i.e.

$$\mathbb{S}_t \mathbb{S}_t^H \quad = \quad I_{2N_{\text{fft}}}, \quad \mathbb{W}_t \mathbb{W}_t^H = I_{2N_{\text{fft}}}. \tag{13}$$

The weighting matrices $\mathbb{X}_{t,m,k}$ and $\mathbb{Y}_{t,m,k}$ in the matrix (9) are real, orthogonal matrices, which always satisfy the following properties for a given value t

$$\mathbb{X}_{t,m,k} \mathbb{X}^H_{t,m,k} = \mathbb{Y}_{t,m,k} \mathbb{Y}^H_{t,m,k} \quad \forall m, k, \tag{14}$$

$$\mathbb{X}_{t,m,k} \mathbb{X}^H_{t,\acute{m},\acute{k}} = -\mathbb{X}_{t,\acute{m},\acute{k}} \mathbb{X}^H_{t,m,k}, \forall \{m,k\} \neq \{\acute{m},\acute{k}\} \tag{15}$$

$$\mathbb{Y}_{t,m,k} \mathbb{Y}^H_{t,\acute{m},\acute{k}} = -\mathbb{Y}_{t,\acute{m},\acute{k}} \mathbb{Y}^H_{t,m,k}, \forall \{m,k\} \neq \{\acute{m},\acute{k}\} \tag{16}$$

$$\mathbb{X}_{t,m,k} \mathbb{Y}^H_{t,\acute{m},\acute{k}} = \mathbb{Y}_{t,\acute{m},\acute{k}} \mathbb{X}^H_{t,m,k} \quad \forall m, k, \acute{m}, \acute{k}. \tag{17}$$

To formulate the ML decoding metric for the symbol $s_{t,m,k}$, for $t = 1, \ldots, (K-1)$, $m = 1, 2$ and $k = 1, \ldots, N_{\text{fft}}$, let us consider the following term

$$D_{m,k} \quad = \quad D^R_{m,k} + iD^I_{m,k}, \tag{18}$$

where $D^R_{m,k} = \Re[\text{tr}(\mathbb{R}_{t-1}\mathbb{R}_t^H \mathbb{X}_{t,m,k})]$ and $D^I_{m,k} = \Re[\text{tr}(\mathbb{R}_{t-1}\mathbb{R}_t^H i\mathbb{Y}_{t,m,k})]$. We have

$$\begin{aligned} D^R_{m,k} &= \Re[\text{tr}(\mathbb{R}_{t-1}\mathbb{R}_t^H \mathbb{X}_{t,m,k})] \\ &= \Re\{\text{tr}[(\mathbb{W}_{t-1}\mathbb{H}_{t-1} + \mathbb{N}_{t-1})(\mathbb{W}_t\mathbb{H}_t + \mathbb{N}_t)^H \mathbb{X}_{t,m,k}]\} \\ &= \Re\{\text{tr}[\big((\mathbb{W}_{t-1}\mathbb{H}_{t-1}\mathbb{H}_t^H\mathbb{W}_{t-1}^H\mathbb{S}_t^H) + \mathbb{N}\big)\mathbb{X}_{t,m,k}]\} \\ &= \Re\{\text{tr}[\big((\mathbb{W}_{t-1}\mathbb{H}_t\mathbb{H}_t^H\mathbb{W}_{t-1}^H\mathbb{S}_t^H) + \mathbb{N}\big)\mathbb{X}_{t,m,k}]\}, \end{aligned} \tag{19}$$

where $\mathbb{N} := \mathbb{W}_{t-1}\mathbb{H}_{t-1}\mathbb{N}_t^H + \mathbb{N}_{t-1}\mathbb{H}_t^H\mathbb{W}_t^H + \mathbb{N}_{t-1}\mathbb{N}_t^H$. The last equality comes from the fact that channel coefficients are constant during the transmission window, i.e. $\mathbb{H}_t = \mathbb{H}_{t-1}$. (This formula indicates that the decoding process is still completely accurate even in the case where the channel changes after every two DSTFC blocks).

Because $\mathbb{S}_t$ and $\mathbb{W}_{t-1}$ are square unitary matrices of size $2N_{\text{fft}}$ (cf. (13)) and $\mathbb{X}_{t,m,k}$ is the weighting matrix of $s^R_{t,m,k}$ (cf. (12)), Eq. (19) becomes

$$D^R_{m,k} = \Re\{\text{tr}[(\mathbb{H}_t\mathbb{H}_t^H)(\mathbb{S}_t^H\mathbb{X}_{t,m,k})]\} + \Re\{\text{tr}(\mathbb{N}\mathbb{X}_{t,m,k})\} \tag{20}$$

The transition from (19) to (20) is detailed in the appendix of this paper. From (12), the first term in (20) is calculated as follows

$$\begin{aligned} &\Re\{\text{tr}[(\mathbb{H}_t\mathbb{H}_t^H)(\mathbb{S}_t^H\mathbb{X}_{t,m,k})]\} = \\ &\quad \frac{1}{\sqrt{2}}\Re\big\{\text{tr}\big[(\mathbb{H}_t\mathbb{H}_t^H)\big(\mathbb{X}^H_{t,m,k}\mathbb{X}_{t,m,k}s^R_{t,m,k} \\ &\quad + \sum_{\forall \acute{m},\acute{k},\{\acute{m},\acute{k}\}\neq\{m,k\}} \mathbb{X}^H_{t,\acute{m},\acute{k}}\mathbb{X}_{t,m,k}s^R_{t,\acute{m},\acute{k}} \\ &\quad + i\sum_{\forall \acute{m},\acute{k}} \mathbb{Y}^H_{t,\acute{m},\acute{k}}\mathbb{X}_{t,m,k}s^I_{t,\acute{m},\acute{k}}\big)\big]\big\}. \end{aligned} \tag{21}$$

It is noted that if Φ is an antihermitian (or skew-Hermitian) matrix, i.e. $\Phi^H = -\Phi$, then $\text{tr}(\mathbb{A}^H\mathbb{A}\Phi)$ is imaginary for any matrix $\mathbb{A}$, thus $\Re\{\text{tr}(\mathbb{A}^H\mathbb{A}\Phi)\} = 0$. From (15), it is easy to check that $(\mathbb{X}^H_{t,\acute{m},\acute{k}}\mathbb{X}_{t,m,k}s^R_{t,\acute{m},\acute{k}})^H = -(\mathbb{X}^H_{t,\acute{m},\acute{k}}\mathbb{X}_{t,m,k}s^R_{t,\acute{m},\acute{k}})$, i.e. $(\mathbb{X}^H_{t,\acute{m},\acute{k}}\mathbb{X}_{t,m,k}s^R_{t,\acute{m},\acute{k}})$ is an antihermitian matrix, thus

$$\Re\{\text{tr}[(\mathbb{H}_t\mathbb{H}_t^H)(\mathbb{X}^H_{t,\acute{m},\acute{k}}\mathbb{X}_{t,m,k}s^R_{t,\acute{m},\acute{k}})]\} = 0, \tag{22}$$

for all $\acute{m}$, $\acute{k}$ and $\{\acute{m},\acute{k}\} \neq \{m,k\}$.

On the other hand, if Θ is a Hermitian matrix, i.e. $\Theta^H = \Theta$, then $\text{tr}(\mathbb{A}^H\mathbb{A}\Theta)$ is real, thus $\Im\{\text{tr}(\mathbb{A}^H\mathbb{A}\Theta)\} = 0$. From (17), it is trivial to realize that $(\mathbb{Y}^H_{t,\acute{m},\acute{k}}\mathbb{X}_{t,m,k}s^I_{t,k})^H = (\mathbb{Y}^H_{t,\acute{m},\acute{k}}\mathbb{X}_{t,m,k}s^I_{t,k})$, i.e. $(\mathbb{Y}^H_{t,\acute{m},\acute{k}}\mathbb{X}_{t,m,k}s^I_{t,k})$ is a Hermitian matrix, thus

$$\begin{aligned} &\Re\{\text{tr}[(\mathbb{H}_t\mathbb{H}_t^H)(i\mathbb{Y}^H_{t,\acute{m},\acute{k}}\mathbb{X}_{t,m,k}s^I_{t,\acute{m},\acute{k}})]\} = \\ &\Im\{\text{tr}[(\mathbb{H}_t\mathbb{H}_t^H)(\mathbb{Y}^H_{t,\acute{m},\acute{k}}\mathbb{X}_{t,m,k}s^I_{t,\acute{m},\acute{k}})]\} = 0 \ \forall m,k,\acute{m},\acute{k}. \end{aligned} \tag{23}$$

If we denote $\mathbb{C}_{t,m,k} := (\mathbb{H}_t\mathbb{H}_t^H)(\mathbb{X}^H_{t,m,k}\mathbb{X}_{t,m,k})$ then $\mathbb{C}_{t,m,k}$ is a constant matrix for given values t, m and k and $\text{tr}(\mathbb{C}_{t,m,k})$ is a positive real number (the trivial case $\text{tr}(\mathbb{C}_{t,m,k}) = 0$ is discarded). From (20)–(23), we have

$$D^R_{m,k} \quad = \quad 1/\sqrt{2}\text{tr}(\mathbb{C}_{t,m,k})s^R_{t,m,k} + \Re\{\text{tr}(\mathbb{N}\mathbb{X}_{t,m,k})\}.$$

The term $D^I_{m,k}$ is calculated in a similar way with the note that (cf. Eq. (14))

$$\mathbb{C}_{t,m,k} = (\mathbb{H}_t\mathbb{H}_t^H)(\mathbb{Y}_{t,m,k}\mathbb{Y}^H_{t,m,k}) = (\mathbb{H}_t\mathbb{H}_t^H)(\mathbb{X}_{t,m,k}\mathbb{X}^H_{t,m,k})$$

we have

$$D^I_{m,k} \quad = \quad 1/\sqrt{2}\ \text{tr}(\mathbb{C}_{t,m,k})s^I_{t,m,k} + \Re\{\text{tr}(\mathbb{N}i\mathbb{Y}_{t,m,k})\}.$$

Therefore

$$\begin{aligned} D_{m,k} = D^R_{m,k} + iD^I_{m,k} = \frac{1}{\sqrt{2}}\text{tr}(\mathbb{C}_{t,m,k})s_{t,m,k} + \\ \Re\{\text{tr}(\mathbb{N}\mathbb{X}_{t,m,k})\} + i\Re\{\text{tr}(\mathbb{N}i\mathbb{Y}_{t,m,k})\}. \end{aligned} \tag{24}$$

The ML decoding metric for $s_{t,m,k}$ can be derived as follows

$$\begin{aligned} \hat{s}_{t,m,k} &= \arg\min |D_{m,k} - \frac{1}{\sqrt{2}}\text{tr}(\mathbb{C}_{t,m,k})s_{t,m,k}|^2 \\ &= \arg\min \big(|D_{m,k}|^2 + \frac{1}{2}[\text{tr}(\mathbb{C}_{t,m,k})]^2|s_{t,m,k}|^2 \\ &- \sqrt{2}\ \text{tr}(\mathbb{C}_{t,m,k})\ \Re\{D^*_{m,k}s_{t,m,k}\}\big) \\ &= \arg\min \big(|D_{m,k}|^2 + \frac{1}{2}[\text{tr}(\mathbb{C}_{t,m,k})]^2 \\ &- \sqrt{2}\ \text{tr}(\mathbb{C}_{t,m,k})\ \Re\{D^*_{m,k}s_{t,m,k}\}\big). \end{aligned} \tag{25}$$

Since $\mathbb{C}_{t,m,k}$ is a constant matrix for given t, m and k and because $\text{tr}(\mathbb{C}_{t,m,k})$ is a positive real number, the equivalent ML decoding metric for $s_{t,m,k}$ is

$$\hat{s}_{t,m,k} \quad = \quad \arg\max_{s_{t,m,k}\in\mathcal{C}} \Re\{D^*_{m,k}s_{t,m,k}\}, \tag{26}$$

for $t = 1, \ldots, (K-1)$, $m = 1, 2$ and $k = 1, \ldots, N_{\text{fft}}$. In fact, there are only $N_D = 100$ data symbols within each MB-OFDM symbol, that include 28 other pilot, guard and null symbols [3]. Therefore, instead of decoding N_{fft} symbols in Eq. (26), i.e. $k = 1, \ldots, N_{\text{fft}}$, we only need to decode N_D symbols, i.e. $k = 1, \ldots, N_D$. The decoding metric (26) holds true for each Rx antenna.

Eq. (26) means that each of the two MB-OFDM symbols $\bar{\mathbf{s}}_{t,1}$ and $\bar{\mathbf{s}}_{t,2}$ can be separately decoded. Furthermore, each symbol $s_{t,m,k}$ within these two MB-OFDM symbols can also be separately decoded based on the above equation. In other words, instead of jointly decoding all $2N_{\text{fft}}$ symbols $s_{t,m,k}$ within the two MB-OFDM symbols $\bar{\mathbf{s}}_{t,1}$ and $\bar{\mathbf{s}}_{t,2}$ at a time, each of them can be separately decoded. No CSI is required for the decoding process. All we need for the decoding process at time t are the received signals at the previous time $(t-1)$ and at the current time. The decoding process is completely linear, thus relatively simple.

B. Dual Carrier Modulation

1) Reviews of DCM [3]: For the data rates higher than 200 Mpbs, DCM, which is a multi-dimensional constellation, will be used instead of QPSK to employ better frequency and time diversities, thus providing better error performance over QPSK. The coded and interleaved binary serial input data shall be divided into groups of 200 bits and converted into

TABLE II
DCM MAPPING TABLE [3]

Input bits	$d[n]$	$d[n+50]$	Input bits	$d[n]$	$d[n+50]$
0000	$-3-3i$	$1+i$	1000	$1-3i$	$3+i$
0001	$-3-1i$	$1-3i$	1001	$1-i$	$3-3i$
0010	$-3+i$	$1+3i$	1010	$1+i$	$3+3i$
0011	$-3+3i$	$1-i$	1011	$1+3i$	$3-i$
0100	$-1-3i$	$-3+i$	1100	$3-3i$	$-1+i$
0101	$-1-i$	$-3-3i$	1101	$3-i$	$-1-3i$
0110	$-1+i$	$-3+3i$	1110	$3+i$	$-1+3i$
0111	$-1+3i$	$-3-i$	1111	$3+3i$	$-1-i$

100 complex numbers. The conversion shall be performed as follows

a) The 200 coded and interleaved bits are grouped into 50 groups of 4 bits. Each group is represented as $(b[g(n)], b[g(n)+1], b[g(n)+50)], b[g(n)+51])$, where $g(n) = 2n$ if $n \in [0, 24]$, and $g(n) = 2n+50$ if $n \in [25, 49]$.
b) Each group of four bits $(b[g(n)], b[g(n)+1], b[g(n)+50)], b[g(n)+51])$ shall be mapped into two different 16-point constellations, i.e. two complex numbers $(d[n], d[n+50])$, separated by 50 tones (sub-carriers). The mapping between bits and constellation is enumerated in Table II.
c) The complex numbers shall be normalized using a normalization factor $1/\sqrt{10}$ to have a unitary normalized average power.

Therefore, after DCM modulation and before OFDM modulation, $N_D = 100$ data symbols are allocated in such a way that the first $N_D/2 = 50$ symbols $s_{t,m,k}$, for $k = 1, \ldots, 50$, are taken from the pool of symbols listed in the 2nd and 5th columns in Table II after being normalized, which is denoted as $\mathcal{C}_{\mathcal{DCM}}$, while the last 50 symbols $s_{t,m,k+50}$ are taken from the pool of symbols listed in the 3rd and 6th columns after being normalized, which is denoted as $\mathcal{C}_{\mathcal{DCM}50}$. It is easy to realize that $|s_{t,m,k}|^2 + |s_{t,m,k+50}|^2 = 2$ for $\forall k, k = 1, \ldots, 50$.

2) Functions of MUX and DEMUX and ML Decoding Method: In the case of DCM, the proposed DSTFC MB-OFDM system comprises two novel blocks, referred to as the multiplexer (MUX) and demultiplexer (DEMUX) (see Fig. 2). Exact functions of these two proposed blocks are explained as follows.

At the transmitter, the MUX block swaps the position of the last 50 data symbols $s_{t,1,k+50}$, for $k = 1, \ldots, 50$, within the MB-OFDM symbol $\bar{\mathbf{s}}_{t,1}$ and that of the first 50 data symbols $s_{t,2,k}$, $k = 1, \ldots, 50$, within the MB-OFDM symbol $\bar{\mathbf{s}}_{t,2}$. By doing this, two new MB-OFDM symbols, denoted as $\bar{\acute{\mathbf{s}}}_{t,1}$ and $\bar{\acute{\mathbf{s}}}_{t,2}$, are generated. Thus we can present $\bar{\acute{\mathbf{s}}}_{t,1}$ and $\bar{\acute{\mathbf{s}}}_{t,2}$ as

$$\begin{aligned}\bar{\acute{\mathbf{s}}}_{t,1} &= [s_{t,1,1}, \ldots, s_{t,1,50},\ s_{t,2,1}, \ldots, s_{t,2,50}]^T,\\ \bar{\acute{\mathbf{s}}}_{t,2} &= [s_{t,1,51}, \ldots, s_{t,1,100},\ s_{t,2,51}, \ldots, s_{t,2,100}]^T.\end{aligned}$$

We denote $\bar{\acute{\mathbf{s}}}_{t,1} = [\acute{s}_{t,1,1}, \ldots, \acute{s}_{t,1,100}]^T$ and $\bar{\acute{\mathbf{s}}}_{t,2} = [\acute{s}_{t,2,1}, \ldots, \acute{s}_{t,2,100}]^T$. It is noted that all symbols within $\bar{\acute{\mathbf{s}}}_{t,1}$ belong to the symbol pool $\mathcal{C}_{\mathcal{DCM}}$, while all symbols within $\bar{\acute{\mathbf{s}}}_{t,2}$ belong to the symbol pool $\mathcal{C}_{\mathcal{DCM}50}$.

Since $|s_{t,m,k}|^2 + |s_{t,m,k+50}|^2 = 2$ for $\forall k, k = 1, \ldots, 50$, one can realize that

$$1/\sqrt{2}\ (|\bar{\acute{\mathbf{s}}}_{t,1}|.\hat{}\,2 + |\bar{\acute{\mathbf{s}}}_{t,2}|.\hat{}\,2) \quad = \quad \bar{\mathbf{1}}.$$

We use the notations $\acute{\mathbb{X}}_{t,m,k}$, $\acute{\mathbb{Y}}_{t,m,k}$ and $\acute{\mathbb{C}}_{t,m,k}$ to denote the matrices that are similar to $\mathbb{X}_{t,m,k}$, $\mathbb{Y}_{t,m,k}$ and $\mathbb{C}_{t,m,k}$ in Section IV-A, but the role of $s_{t,m,k}$ has been replaced by $\acute{s}_{t,m,k}$. By the proposed structure, the following three conditions have always been assured

a) The normalized transmitted matrix $\mathbb{S}_t$ in the DCM case

$$\mathbb{S}_t \quad = \quad 1/\sqrt{2}\begin{bmatrix} \mathrm{diag}(\bar{\acute{\mathbf{s}}}_{t,1}) & \mathrm{diag}(\bar{\acute{\mathbf{s}}}_{t,2}) \\ -\mathrm{diag}(\bar{\acute{\mathbf{s}}}^*_{t,2}) & \mathrm{diag}(\bar{\acute{\mathbf{s}}}^*_{t,1}) \end{bmatrix}$$

satisfies $\mathbb{S}_t\mathbb{S}_t^H = I_{2N_{\mathrm{fft}}}$, similarly to (13).
b) The equality $\acute{\mathbb{C}}_{t,1,k} = \acute{\mathbb{C}}_{t,2,k}$, i.e. $\acute{\mathbb{X}}^H_{t,1,k}\acute{\mathbb{X}}_{t,1,k} = \acute{\mathbb{X}}^H_{t,2,k}\acute{\mathbb{X}}_{t,2,k} = \acute{\mathbb{Y}}^H_{t,1,k}\acute{\mathbb{Y}}_{t,1,k} = \acute{\mathbb{Y}}^H_{t,2,k}\acute{\mathbb{Y}}_{t,2,k}$, is guaranteed for $\forall t, k$. We denote $\acute{\mathbb{C}}_{t,k} := \acute{\mathbb{C}}_{t,1,k} = \acute{\mathbb{C}}_{t,2,k}$.
c) We always have $\frac{1}{2}(|\acute{s}_{t,1,k}|^2 + |\acute{s}_{t,2,k}|^2) = 1\ \forall k, k = 1, \ldots, 100$.

As a result, each pair of symbols $(\acute{s}_{t,1,k}, \acute{s}_{t,2,k})$, for $k = 1, \ldots, 100$, within the pair of MB-OFDM symbols $(\bar{\acute{\mathbf{s}}}_{t,1}, \bar{\acute{\mathbf{s}}}_{t,2})$ can be decoded separately based on the following ML decoding metric, which is achieved by a slight modification of the ML decoding metric (25) in Section IV-A:

$$\begin{aligned}&(\hat{\acute{s}}_{t,1,k}, \hat{\acute{s}}_{t,2,k})\\ &= \arg\min \sum_{m=1}^{2} \left|D_{m,k} - \frac{1}{\sqrt{2}}\mathrm{tr}(\acute{\mathbb{C}}_{t,m,k})\acute{s}_{t,m,k}\right|^2\\ &= \arg\min \Bigg[\sum_{m=1}^{2}|D_{m,k}|^2 + \frac{1}{2}[\mathrm{tr}(\acute{\mathbb{C}}_{t,k})]^2\sum_{m=1}^{2}|\acute{s}_{t,m,k}|^2\\ &\quad - \sqrt{2}\mathrm{tr}(\acute{\mathbb{C}}_{t,k})\sum_{m=1}^{2}\Re\{D^*_{m,k}\acute{s}_{t,m,k}\}\Bigg]\\ &= \arg\min \Bigg[\sum_{m=1}^{2}|D_{m,k}|^2 + [\mathrm{tr}(\acute{\mathbb{C}}_{t,k})]^2\\ &\quad - \sqrt{2}\mathrm{tr}(\acute{\mathbb{C}}_{t,k})\sum_{m=1}^{2}\Re\{D^*_{m,k}\acute{s}_{t,m,k}\}\Bigg].\end{aligned}$$

In these formulas, $D_{m,k}$ is calculated in the similar manner as (18) with the role of $s_{t,m,k}$ substituted by $\acute{s}_{t,m,k}$. The above metric is equivalent to the following one

$$(\hat{\acute{s}}_{t,1,k}, \hat{\acute{s}}_{t,2,k}) = \arg \max_{\substack{\acute{s}_{t,1,k} \in \mathcal{C}_{\mathcal{DCM}} \\ \acute{s}_{t,2,k} \in \mathcal{C}_{\mathcal{DCM}50}}} \Re\{D^*_{1,k}\acute{s}_{t,1,k} + D^*_{2,k}\acute{s}_{t,2,k}\} \tag{27}$$

for $\forall k, k = 1, \ldots, 100$. The decoding metric (27) can be applied to any Rx antenna.

After all data symbols within the two MB-OFDM symbols $\bar{\acute{\mathbf{s}}}_{t,1}$ and $\bar{\acute{\mathbf{s}}}_{t,2}$ are decoded, the DEMUX block swaps back the position of the last 50 data symbols in $\bar{\acute{\mathbf{s}}}_{t,1}$ and that of the first 50 data symbols in $\bar{\acute{\mathbf{s}}}_{t,2}$. Thereby, the MB-OFDM symbols $\bar{\mathbf{s}}_{t,1}$ and $\bar{\mathbf{s}}_{t,2}$ have been completely decoded.

Comparing (26) and (27), one can realize that decoding DSTFCs in the DCM case is slightly more complicated than that in the PSK or 4QAM case, though decoding complexity in both cases is relatively simple.

To this point, we have derived the decoding metrics for the proposed DSTFC MB-OFDM system in both scenarios of constant envelop modulation and multi-dimensional modulation schemes with one Rx antennas. Generalization for the case

of an arbitrary number N of Rx antennas will be mentioned shortly in the next section.

V. Performance Analysis

In this section, we first derive the pairwise error probability (PEP) of the proposed DSTFC MB-OFDM system in Section V-A. The maximum achievable diversity order of the proposed system is then evaluated in Section V-B for both scenarios of constant envelope modulation schemes and the DCM scheme. Finally, an in-depth analysis of the factors affecting to the realistic system error performance is mentioned in Section V-C. This in-depth analysis indicates that the value of the diversity order calculated in Section V-B should only be used as the coarse indicator, rather than a fine measure, for the improvement of the system error performance.

It is noted that the maximum diversity order defined in this paper (similarly to that in [7]) is the maximum diversity order of the signals at the output of the OFDM demodulation block (cf. Fig. 1 or Fig. 2). The maximum diversity order of the signals arriving at the Rx antennas (before the OFDM demodulation block, calculated by Eq. (1)) could be very large due to the rich dispersion of UWB channels (the average number of multipaths may reach some thousands). However, the maximum diversity order of the signals at the output of the OFDM demodulation block is limited because the FFT size, $N_{\text{fft}} = 128$, is very limited, compared to the full length of UWB multipaths. Thus the maximum diversity order of the outgoing signals from the OFDM demodulation block should be examined, rather than the arriving signals at the Rx antennas. The former represents the effect of an important technical specification of the system, i.e. the limited FFT size of the OFDM demodulation block, while the latter does not reflect the essence of the effect of the FFT operation to the diversity order.

A. Pairwise Error Probability

Denote E_s to be the average energy of the signal constellation. For the Alamouti STFC $\mathbf{S}_t$ in (8), both the number of MB-OFDM symbol time slots required to transmit the whole block, denoted as T, and the number of Tx antennas, M, are equal to 2, i.e. $T = M = 2$. We consider the probability that a ML receiver decides erroneously in favor of a signal

$$\mathbf{e} = [e_{1,1,1} \dots e_{1,1,N_{\text{fft}}}, \dots, e_{T,M,1} \dots e_{T,M,N_{\text{fft}}}],$$

assuming that

$$\mathbf{c} = [c_{1,1,1} \dots c_{1,1,N_{\text{fft}}}, \dots, c_{T,M,1} \dots c_{T,M,N_{fft}}]$$

was transmitted. Note that each group of N_{fft} consecutive data inside $\mathbf{c}$ in fact forms a certain vector $\bar{\mathbf{s}}$ in the matrix $\mathbf{S}_t$ defined in (8).

From (11), the received signal matrices during the two time instants t and $(t-1)$ can be written as

$$\mathbb{R}_{t-1} = \mathbb{H}_{t-1}\mathbb{W}_{t-1} + \mathbb{N}_{t-1}$$

$$\mathbb{R}_t = \mathbb{H}_t\mathbb{W}_{t-1}\mathbb{S}_t + \mathbb{N}_t = \mathbb{R}_{t-1}\mathbb{S}_t + (\mathbb{N}_t - \mathbb{N}_{t-1}\mathbb{S}_t), \quad (28)$$

where the last equality comes from the fact that $\mathbb{H}_{t-1} = \mathbb{H}_t$. If N_0 is the variance of the Gaussian noise entries in $\mathbb{N}_{t-1}$ and $\mathbb{N}_t$, given that $\mathbb{S}_t$ is an unitary matrix, it is easy to realize that the variance of the noise term $(\mathbb{N}_t - \mathbb{N}_{t-1}\mathbb{S}_t)$ is $2N_0$. It is also noted that $\mathbb{R}_{t-1}$ and $\mathbb{R}_t$ are the matrices of the received signals, thus they are known (i.e. constant). The ML decoding metric for the transmitted matrix $\mathbb{S}_t$, given that $\mathbb{R}_{t-1}$ and $\mathbb{R}_t$ are known at the receiver, becomes

$$\hat{\mathbb{S}}_t = \arg \min_{\mathbb{S}_t \in \mathcal{C}^{2N_{\text{fft}}}} \|\mathbb{R}_t - \mathbb{R}_{t-1}\mathbb{S}_t\|_F^2, \quad (29)$$

where $\mathcal{C}^{2N_{\text{fft}}}$ denotes all possibilities of values that the matrix $\mathbb{S}_t$ could take, and $\|.\|_F$ denotes the Frobenius norm. It should be emphasized that (29) is in fact the most general form of the decoding metric in (26) because we can further write (29) as follows

$$\begin{aligned}\hat{\mathbb{S}}_t &= \arg \min_{\mathbb{S}_t \in \mathcal{C}^{2N_{\text{fft}}}} \|\mathbb{R}_t - \mathbb{R}_{t-1}\mathbb{S}_t\|_F^2, \\ &= \arg \min_{\mathbb{S}_t \in \mathcal{C}^{2N_{\text{fft}}}} \text{tr}\big[(\mathbb{R}_t - \mathbb{R}_{t-1}\mathbb{S}_t)^H(\mathbb{R}_t - \mathbb{R}_{t-1}\mathbb{S}_t)\big], \\ &= \arg \max_{\mathbb{S}_t \in \mathcal{C}^{2N_{\text{fft}}}} \Re\big\{\text{tr}(\mathbb{R}_t^H\mathbb{R}_{t-1}\mathbb{S}_t)\big\}.\end{aligned}$$

Equations (28) and (29) indicate that, given the received signal matrices $\mathbb{R}_{t-1}$ and $\mathbb{R}_t$ in the two time instants $(t-1)$ and t, the performance analysis of the proposed system can be turned into the performance analysis of the coherent STFC MB-OFDM UWB system which has been analyzed in [7], by replacing the role of the channel matrix $\mathbb{H}_t$ in the coherent system by the received matrix $\mathbb{R}_{t-1}$ in the differential system, and by noting that the noise variance in the differential system is twice that in the coherent system. Additionally, at high signal-to-noise ratio (SNR), we have $\mathbb{R}_{t-1} \approx \mathbb{H}_t\mathbb{W}_{t-1}$. If $\mathbb{H}_t$ contains log-normally distributed random variables, so does $\mathbb{R}_{t-1}$ (it has been proved in [7, Section IV] that the weighted sum of a finite number of log-normally distributed random variables can be well approximated by another log-normally distributed random variable). Therefore, an approach similar to that mentioned in [7, Section IV] for a coherent STFC MB-OFDM UWB system is adopted for the proposed DSTFC MB-OFDM UWB system, resulting in the Chernoff bound of the pairwise error probability in *log-normally* distributed fading channels at a *high* SNR as follows

$$\begin{aligned}P(\mathbf{c} \to \mathbf{e}) \leq &\Bigg[\big(E_s/8N_0\big)^{-rNN_{\text{fft}}}\Big(\prod_{k=1}^{N_{\text{fft}}}\prod_{m=1}^{r}\lambda_{m,k}\Big)^{-N} \\ &\prod_{n=1}^{N}\prod_{k=1}^{N_{\text{fft}}}\prod_{m=1}^{r}\exp(-K_{m,n,k})\Bigg], \quad (30)\end{aligned}$$

where $r = \min\{r_k\}$, and r_k, for $k = 1, \dots, N_{\text{fft}}$, is the rank of matrix $\mathbf{B}_k(\mathbf{c}, \mathbf{e})$, which is defined as

$$\mathbf{B}_k(\mathbf{c}, \mathbf{e}) = \begin{bmatrix} c_{1,1,k} - e_{1,1,k} & \dots & c_{1,M,k} - e_{1,M,k} \\ c_{2,1,k} - e_{2,1,k} & \dots & c_{2,M,k} - e_{2,M,k} \\ \dots & \dots & \dots \\ c_{T,1,k} - e_{T,1,k} & \dots & c_{T,M,k} - e_{T,M,k} \end{bmatrix},$$

$\lambda_{m,k}$ are the eigenvalues of $\mathbf{B}_k(\mathbf{c}, \mathbf{e})^H\mathbf{B}_k(\mathbf{c}, \mathbf{e})$, which are nonnegative real numbers, and $K_{m,n,k}$ is a term depending on the distribution parameters of the log-normally distributed random variables in the matrix $\mathbb{R}_{t-1}$.

Recall that the Chernoff bound for the pairwise error probability of a coherent STFC MB-OFDM UWB system in

$$\mathbb{H}_t\mathbb{H}_t^H = \begin{bmatrix} \sum_n^N |\hbar_{t,1,n,1}|^2 & & & & \cdots & \cdots & \cdots \\ & \ddots & & & & \cdots & \cdots \\ & & \sum_n^N |\hbar_{t,1,n,N_{\text{fft}}}|^2 & & & & \cdots \\ \cdots & & & \sum_n^N |\hbar_{t,2,n,1}|^2 & & & \\ & & & & & \ddots & \\ \cdots & \cdots & & & & & \\ \cdots & \cdots & \cdots & & & & \sum_n^N |\hbar_{t,2,n,N_{\text{fft}}}|^2 \end{bmatrix}$$

log-normally distributed fading channels at a *high* SNR is (cf. (34) in [7])

$$P(\mathbf{c}\to\mathbf{e}) \leq \left[\left(E_s/4N_0\right)^{-rNN_{\text{fft}}}\left(\prod_{k=1}^{N_{\text{fft}}}\prod_{m=1}^{r}\lambda_{m,k}\right)^{-N} \prod_{n=1}^{N}\prod_{k=1}^{N_{\text{fft}}}\prod_{m=1}^{r}\exp(-K_{m,n,k})\right]. \quad (31)$$

Equations (30) and (31) indicate that, if SNR is large enough, the differential system behaves similarly to the coherent STFC MB-OFDM UWB system, except for the fact that the former is inferior by approximate 3dB, compared to the latter, due to the noise variance is double in the differential system. This observation will be confirmed by simulation results mentioned later in this paper. This observation is similar to the observation in a differential space-time coded system in Rayleigh fading channels, where the Chernoff bound is the same as that in the coherent space-time coded system (with perfect CSI at the receiver), except for a 3-dB loss in SNR [29, Sections III.B].

The aforementioned analysis is derived regardless of a specific modulation scheme, thus it can be applied to different modulation schemes (M-PSK, 4-QAM or DCM).

B. Diversity Order

In this subsection, the diversity order of the proposed Alamouti DSTFC MB-OFDM system, i.e. $M = 2$, will be derived for an arbitrary number N of Rx antennas in both scenarios of constant envelope modulation and DCM schemes.

From (30), it is intuitive that a diversity order of rNN_{fft} and a coding gain (over a differential MB-OFDM UWB system without space-time-frequency codes) of

$$\left(\prod_{k=1}^{N_{\text{fft}}}\prod_{m=1}^{r}\lambda_{m,k}\right)^{-N}\prod_{n=1}^{N}\prod_{k=1}^{N_{\text{fft}}}\prod_{m=1}^{r}\exp(-K_{m,n,k})$$

could be achieved. The maximum achievable diversity order of the proposed system is achieved when $r = M$, thus the maximum achievable diversity order is MNN_{fft}.

Alternatively, one can also work out the system diversity order based on the decoding metric in (24). Basic idea for this approach is that diversity order is the number of independent fading coefficients that can be averaged over to detect the symbol [30, Section II.B], [31, Section IV]. To derive the diversity order using this approach, we first generalize Eq. (24) for the case of N Rx antennas. In this case, the channel matrix is denoted as (cf. Eq.(7))

$$\mathbb{H}_t = \{\text{diag}(\bar{\mathfrak{h}}_{t,m,n})\}_{2N_{\text{fft}}\times NN_{\text{fft}}}, \quad (32)$$

where the subscript n indicates the n-th Rx antenna ($n = 1,\ldots,N$), and

$$\bar{\mathfrak{h}}_{t,m,n} = \text{FFT}\{\bar{\mathbf{h}}_{t,m,n}\} = [\hbar_{t,m,n,1}\ \hbar_{t,m,n,2}\ldots\hbar_{t,m,n,N_{\text{fft}}}]^T \quad (33)$$

From (32) and (33), $\mathbb{H}_t\mathbb{H}_t^H$ is a square matrix of size $2N_{\text{fft}}\times 2N_{\text{fft}}$ having the $[(m-1)N_{\text{fft}}+p]$-th element, for $m = 1, 2$ and $p = 1,\ldots,N_{\text{fft}}$, on its main diagonal to be $\sum_n^N |\hbar_{t,m,n,p}|^2$. In other words, the main diagonal of $\mathbb{H}_t\mathbb{H}_t^H$ has the form shown on the top of this page. Other elements of this matrix might not be zeros. Meanwhile, for the Alamouti DSTFC in (9), it is easy to realize that $\mathbb{X}_{t,m,k}^H\mathbb{X}_{t,m,k}$ is the square matrix of size $2N_{\text{fft}}\times 2N_{\text{fft}}$, which contains only two numbers of one at the k-th and $(N_{\text{fft}}+k)$-th positions in its main diagonal. All other elements of this matrix are zeros. Therefore, we have

$$\begin{aligned}\text{tr}(\mathbb{C}_{t,m,k}) &= \text{tr}\left[(\mathbb{H}_t\mathbb{H}_t^H)(\mathbb{X}_{t,m,k}^H\mathbb{X}_{t,m,k})\right] \\ &= \sum_n^N\left[|\hbar_{t,1,n,k}|^2 + |\hbar_{t,2,n,k}|^2\right]. \quad (34)\end{aligned}$$

Substitute (34) into (24), the metric $D_{m,k}$ for the case of N Rx antennas can be written as

$$\begin{aligned}D_{m,k} &= \frac{1}{\sqrt{2}}\sum_n^N\sum_{m=1}^{2}|\hbar_{t,m,n,k}|^2 s_{t,m,k} + \\ &\quad \Re\{\text{tr}(\mathbb{N}\mathbb{X}_{t,m,k})\} + i\Re\{\text{tr}(\mathbb{N}i\mathbb{Y}_{t,m,k})\}. \quad (35)\end{aligned}$$

It has been proved in our previous work [7] that the N_{fft}-point FFT of a channel vector $\bar{\mathbf{h}}_{t,m,n}$ consisting of $L_{t,m,n}$ ($L_{t,m,n} > N_{\text{fft}}$) real multipath components $h_{t,m,n,l}$ (for $l = 1,\ldots,L_{t,m,n}$), whose magnitudes are independently log-normally distributed RVs, results in a channel vector $\bar{\mathfrak{h}}_{t,m,n}$ consisting of N_{fft} complex multipath components $\hbar_{t,m,n,k}$ (for $k = 1,\ldots,N_{\text{fft}}$), which are also independently log-normally distributed RVs. It is emphasized that if the FFT size N_{ftt} is not smaller than the average number of multipath components $\bar{N}_p$ (which is usually not the case of MB-OFDM UWB systems), then the N_{fft}-point FFT of $\bar{\mathbf{h}}_{t,m,n}$ results in a vector $\bar{\mathfrak{h}}_{t,m,n}$ consisting of $\bar{N}_p$, rather than N_{fft}, independently log-normally distributed RVs. Further, it has been proved there that if $\hbar_{t,m,n,k}$ ($k = 1,\ldots,N_{\text{fft}}$) are independently log-normally distributed RVs, then $|\hbar_{t,m,n,k}|^2$ are also independently log-normally distributed RVs. Interested readers may refer to Section IV in [7] for more detail.

From (35), the equivalent channel gain $\left(\frac{1}{\sqrt{2}}\sum_n^N\sum_{m=1}^{2}|\hbar_{t,m,n,k}|^2\right)$ for the symbol $s_{t,m,k}$ corresponding to the k-th subcarrier is a function of $2N$ RVs $|\hbar_{t,m,n,k}|^2$, i.e. it has $2N$ degrees of freedom. In other words, the decoding metric for an arbitrary MB-OFDM

symbol $\bar{\mathbf{s}}_{t,m} = [s_{t,m,1} \quad s_{t,m,2} \ldots s_{t,m,N_{\text{fft}}}]^T$ within the transmitted space-time-frequency code in (8) has $2NN_{\text{fft}}$ degrees of freedom. The factor 2 in the formula $2NN_{\text{fft}}$ is actually the number of Tx antennas. Generalization for an arbitrary number of Tx antennas M is thus trivial, and the diversity order of DSTFC MB-OFDM UWB systems is MNN_{fft}.

In [7], we have proved that the maximum achievable diversity order of a (coherent) STFC MB-OFDM system is MNN_{fft}. This means that the proposed space-time-frequency processing concept for MB-OFDM UWB systems possesses the diversity order of MNN_{fft}, regardless of coherent or non-coherent detection. It should be emphasized that though they have the same diversity orders, the differential detection is inferior by approximate 3 dB compared to the coherent detection as the penalty of missing the exact CSI at the receiver. This finding is consistent with the well-known knowledge in a *conventional* wireless system that the diversity orders of the system are the same in coherent and differential detections, and that the gap between the system performances is approximate 3 dB [29, Sections III,IV], [31, Section V], [32, Fig.1], [33, Fig.1].

Interestingly, the diversity order of MNN_{fft} found in this paper (and in [7]) for the proposed system in *log-normally* distributed fading channels agrees with the finding in [6] for the coherent MB-OFDM MIMO UWB system in *Nakagami-m* fading channels. (In [6], the diversity order was found to be $\min(LN_{\text{fft}}MN, KN_{\text{fft}}N)$, where K denotes the number of jointly encoded OFDM symbols, which is in turn equal to M for a full rate code, such as the Alamouti code. Given that L, which is the number of multipaths, is extremely large for an UWB system, the diversity order becomes MNN_{fft}).

An interesting observation can be drawn from (35) is that the equivalent channel gain $\left(\frac{1}{\sqrt{2}}\sum_n^N \sum_{m=1}^2 |\hbar_{t,m,n,k}|^2\right)$ for each transmitted symbol $s_{t,m,k}$ is the sum of N equivalent gains $\frac{1}{\sqrt{2}}\sum_{m=1}^2 |\hbar_{t,m,n,k}|^2$ created by individual Rx antennas. This observation allows the decoding process to be further simplified by just calculating the decoding metric, denoted as $D_{m,n,k}$ (the subscript n indicates the n-th Rx antenna), based on (18) as if the system merely had one Rx antenna (the n-th Rx antenna)

$$D_{m,n,k} = D^R_{m,n,k} + iD^I_{m,n,k} = \Re[\text{tr}(\mathbb{R}_{t-1,n}\mathbb{R}^H_{t,n}\mathbb{X}_{t,m,k})] + i\Re[\text{tr}(\mathbb{R}_{t-1,n}\mathbb{R}^H_{t,n}i\mathbb{Y}_{t,m,k})],$$

and then adding the effect of all individual decoding metrics $D_{m,n,k}$ for N Rx antennas to decode the symbol $s_{t,m,k}$ by the following formula

$$\hat{s}_{t,m,n,k} = \arg \max_{s_{t,m,k}\in\mathcal{C}} \sum_{n=1}^{N} \Re\{D^*_{m,n,k}s_{t,m,k}\}.$$

In the similar manner, the decoding metric for the DCM scheme in the case of N Rx antennas can be expressed as follows

$$(\hat{\acute{s}}_{t,1,k}, \hat{\acute{s}}_{t,2,k}) = \arg \max_{\substack{\acute{s}_{t,1,k}\in\mathcal{C}_{\mathcal{DCM}} \\ \acute{s}_{t,2,k}\in\mathcal{C}_{\mathcal{DCM}50}}} \sum_{n=1}^{N} \Re\{D^*_{1,n,k}\acute{s}_{t,1,k} + D^*_{2,n,k}\acute{s}_{t,2,k}\},$$

for $\forall k, k = 1, \ldots, 100$.

This observation allows us to basically "clone" the Matlab programming cell for decoding symbols in the system with only one Rx antennas to N similar cells (with slight modifications) to cover the case of N Rx antennas. Hence, the decoding complexity in the case of N Rx antennas is only slightly increased, compared to the case of one Tx antenna.

C. Comments on Realistic System Performance

Section V-B has quantified the maximum achievable diversity order of the proposed DSTFC MB-OFDM system to be MNN_{fft}. One may have a question about whether the performances of a system with given values of M, N and N_{fft} would be the same in different channel models CM1-CM4, having known that the system has the same maximum achievable diversity order in all channel models.

The answer for this question is that the performances of the same system are different in different channel models. Simulation results in this paper shall clearly show that the more dispersive the channel is, the worse the system error performance is. In other words, the slope of the system bit error curve is reduced for a more dispersive channel model. This phenomenon is due to the affect of the following two un-ideal factors to the performance of a realistic MB-OFDM UWB system.

1) Limited Length of ZPS: Theoretically, it is well known in an OFDM-based system that the length of ZPS (or cyclic prefix (CP)) must not be shorter than the longest multipath channel to turn the linear convolution (cf. Eq. (1)) between the transmitted signal and the channel vector into the circular convolution (cf. Eq. (2)), thus facilitating an accurate signal recovery in the frequency domain using a FFT operation. If it is not the case, the energy of multipath components within the ZPS (or CP) window will be captured, while that of the multipath components outside this window will be discarded. This results in a loss of useful signal power. Unfortunately, this situation normally holds for MB-OFDM UWB systems where the channels are very dispersive with the average number of multipaths $\bar{N}_p$ being much bigger than $N_{ZPS} = 37$ (see Table I). Consequently, in a realistic MB-OFDM UWB system, ZPS can partially, but not completely, capture the useful signal power which is required for the accurate signal recovery. Mathematically speaking, the circular convolution in (3) is not exactly equal to, but approximate the first N_{fft} samples achieved by the OAAO of the linear convolution $\bar{\mathbf{x}}_{ZP,t,m} * \bar{\mathbf{h}}_{m,n}$ in (1). In other words, the transition from (1) to (2) is an approximation, rather than an exact match. The difference between (1) and (2) is larger when the channel is more dispersive and/or the SNR is higher (since a higher transmitted power causes a higher power loss). Therefore, there exits a gap between the ideal system performance (i.e. when N_{ZPS} is larger than the largest number of channel multipaths) and the system performance when realistic channel conditions and the limited length of ZPS are taken into account. The difference between the ideal system performance and the realistic system performance increases if the channel is more dispersive. As a result, the more dispersive the channel is, the worse the performance of a realistic MB-OFDM system

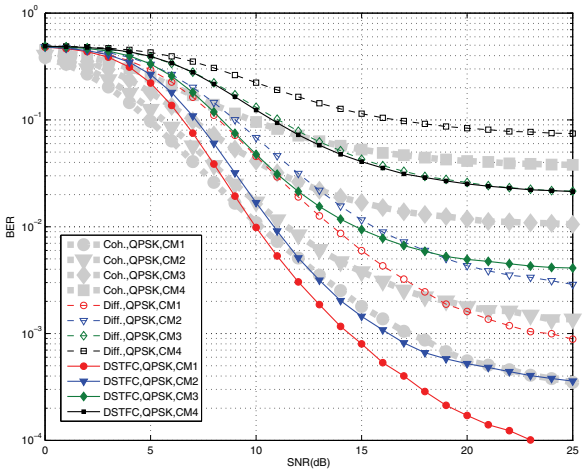

Fig. 3. DSTFC MB-OFDM vs. differential MB-OFDM (without STFCs) and coherent MB-OFDM (without STFCs) with QPSK modulation in the case of one Rx antenna.

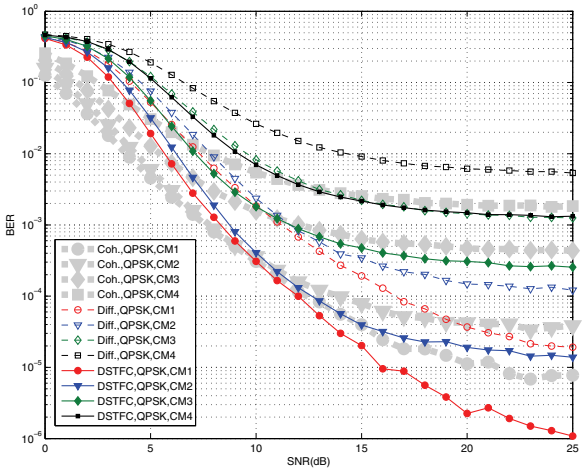

Fig. 4. DSTFC MB-OFDM vs. differential MB-OFDM and coherent MB-OFDM with QPSK modulation in the case of two Rx antennas.

is. The slope of the bit error curve reduces for a more dispersive channel model.

2) Limited FFT/IFFT Size: It is easy to realize that, for a given N_{fft}, the N_{ftt}-point FFT of the channel vectors $\bar{\mathbf{h}}_{m,n} = [h_{m,n,1},\ h_{m,n,2}, \ldots,\ h_{m,n,L_{m,n}}]^T$, i.e. FFT$\{\bar{\mathbf{h}}_{m,n}\}$, of different lengths $L_{m,n}$ always provides the same result, as long as $L_{m,n}$ is not smaller than N_{fft}. This means that, by FFT-ing the received signals with a *limited* FFT size N_{fft} following Eq. (3), the N_{fft}-point FFT operation truncates the impact of a long vector $\bar{\mathbf{h}}_{m,n}$ to the length of N_{fft}. (This observation also explains intuitively why the diversity order of a received MB-OFDM symbol is MNN_{fft} as mentioned in Section V-B, rather than MNL_{max}, where L_{max} denotes the biggest number of multipaths among the MB-OFDM UWB channels). This is the second reason for the mismatch between the linear convolution in (1) and the circular convolution in (2) in a realistic MB-OFDM UWB system. The truncating

TABLE III
SIMULATION PARAMETERS.

Parameter	Value
FFT and IFFT size	$N_{\text{fft}} = 128$
Data rate	320 Mbps
Convolutional encoder's rate	1/2
Convolutional encoder's constraint length	7
Convolutional decoder	Viterbi
Decoding mode	Hard
STFC decoding at nodes	ML decoding
Number of transmitted DSTFC blocks	1200
Modulation	QPSK, DCM
IEEE Channel model	CM1, 2, 3 & 4
Number of data subcarriers	$N_D = 100$
Number of pilot subcarriers	$N_P = 12$
Number of guard subcarriers	$N_G = 10$
Total number of subcarriers used	$N_T = 122$
Number of samples in ZPS	$N_{ZPS} = 37$
Total number of samples/symbol	$N_{SYM} = 165$
Number of channel realizations	100

effect also causes a certain loss of the useful power since the signal power received via various other channel multipaths is not considered. This power loss is bigger when SNR increases (since the useful power which is not taken into account is higher when the transmitted power is higher). Clearly, the higher N_{fft} is, the better the full impact of the multipath channel is reflected, and thus the better the system performance is. (This analysis will be further verified by the simulation results in Section VI). However, FFT and IFFT blocks significantly decide the complexity and the cost of transmitter and receiver. In a realistic MB-OFDM UWB system [3], [4], the FFT/IFFT size is $N_{\text{fft}} = 128$, which is typically much smaller than the length of UWB channels. As a result, there is a compromise between the cost/complexity and the system performance.

Due to the aforementioned reasons, the BER (bit-error-rate) curves of a realistic MB-OFDM system for different channel models CM1-CM4 are expected not to be parallelled. The above reasons provide the insight of the fact that a DSTFC MB-OFDM system with given numbers of Tx and Rx antennas and given N_{fft} performs differently in different channel models CM1-CM4, despite that the system has the same maximum diversity order in all four channel models. Specifically, the more dispersive the channel is, the worse the system performance is, and thus the smaller the slope of the BER curve is. This observation will be confirmed by simulations in the next section. Therefore, it is recommended that the diversity order quantified in Section V-B should only be considered as a raw indicator, rather than an exact measure, of the possible enhancement of the system performance.

VI. SIMULATION RESULTS

To examine the performance advantage of the proposed DSTFC MB-OFDM system, several Monte-Carlo simulations were run in Matlab for four systems, namely the baseband, conventional differential MB-OFDM system (without MIMO) with QPSK modulation, the baseband, conventional coherent MB-OFDM system (without MIMO) with QPSK modulation, and the two baseband Alamouti DSTFC MB-OFDM systems with QPSK and DCM schemes.

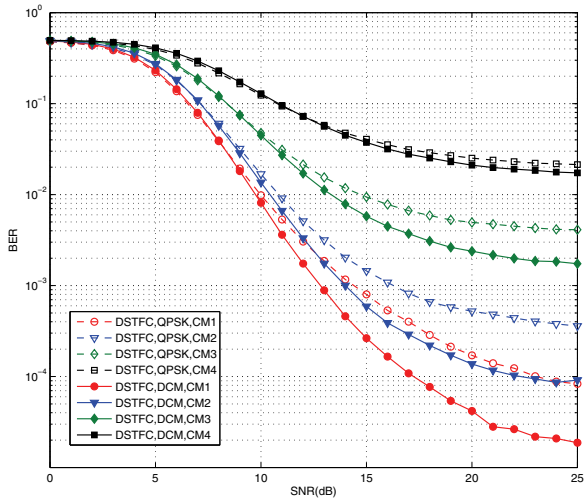

Fig. 5. DSTFC MB-OFDM with DCM vs. DSTFC MB-OFDM with QPSK in the case of one Rx antenna.

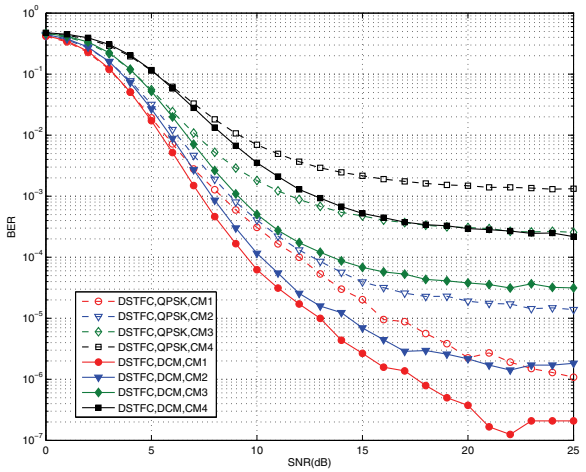

Fig. 6. DSTFC MB-OFDM with DCM vs. DSTFC MB-OFDM with QPSK in the case of two Rx antennas.

TABLE IV
SLOPES OF BER CURVES BETWEEN $BER = 10^{-1}$ AND $BER = 10^{-2}$.

Differential transmission	CM1	CM2	CM3	CM4
no MIMO ($\triangle SNR$ dB/BER decade)	0.65	0.71	0.82	1.18
MIMO ($\triangle SNR$ dB/BER decade)	0.47	0.53	0.59	0.76

The conventional differential MB-OFDM system was simply created in a similar way as Eq. (10), but it was much more simplified because transmission was carried out in a symbol-by-symbol basis rather than a block-by-block basis as in a DSTFC MB-OFDM system. In particular, the transmitted MB-OFDM symbol at time t is the Hadamard product of the transmitted symbol at time $t-1$ and a new information symbol. The initial transmitted symbol is set to the vector $\bar{\mathbf{1}}$. Decoding process was also carried out in a similar manner to Eq. (26).

Each run of simulations was carried out with 1,200 Alamouti DSTFC blocks. One hundred channel realizations of each channel model (CM1 to CM4) were considered for the transmission of each DSTFC block. The channel realizations were created by the Matlab program enclosed in the appendix of the IEEE 802.15.3a channel modeling sub-committee report [21]. In simulations, SNR is defined to be the signal-to-noise ratio (dB) per sample in a MB-OFDM symbol (consisting of 165 samples) at each Rx antenna (i.e. the subtraction between the total power (dB) of the received signal corresponding to the sample of interest and the power of noise (dB) at that Rx antenna). All systems were considered at the bit rate 320 Mbps. Further, the total average powers transmitted from all Tx antennas are equal in all four systems at any time, in order to fairly compare their performances. The complete set of simulation parameters is presented in Table III.

Fig. 3 compares the bit error performance of the three systems, namely the conventional differential MB-OFDM (dashed curves), the conventional coherent MB-OFDM (shaded curves), and the Alamouti DSTFC MB-OFDM (solid curves), in the case where the receiver is equipped with only one Rx antenna. From this figure, the proposed DSTFC MB-OFDM system brings about a significant improvement in the bit error performance, compared to the other two MB-OFDM systems. For instance, the Alamouti DSTFC provides approximately a 3.5 dB gain in CM1 at the bit error rate $BER = 10^{-2}$, compared to the conventional differential MB-OFDM. The more dispersive the channel is (CM1 is the least dispersive channel model while CM4 is the most dispersive one), the higher gain the DSTFC provides. Furthermore, the proposed DSTFC system can even provide much better bit error performance over the conventional coherent MB-OFDM system at high SNRs. For example, the former is better than the latter at SNR being higher than 10 dB in CM1 and the gain can be as large as 2.5 dB at $BER = 10^{-3}$. This improvement is due to the fact that the former deploys the MIMO system (more accurately, the 2×1 MIMO model).

Fig. 4 presents the bit error performance of the three systems in the case of two Rx antennas, i.e. in a 2×2 MIMO model. Once again, we can see that DSTFCs improve significantly the bit error performance of MB-OFDM systems. For illustration, a gain of at least 4.5 dB (over the conventional differential MB-OFDM system) can be achieved at $BER = 10^{-4}$ when the Alamouti DSTFC is utilized. Similarly, the DSTFC system might even perform much better than the conventional coherent MB-OFDM system at the high SNR range. It is noted that the aforementioned improvements were gained without any increase of total transmission power, but thanks to the introduced space, time and frequency diversities in the proposed DSTFC MB-OFDM system.

From the two figures, one can observe the error performance enhancement in the Alamouti DSTFC system, compared to the conventional differential MB-OFDM system, in all channel models thanks to the higher diversity order introduced by the proposed DSTFC MB-OFDM system. For illustration, the slopes of BER curves of the two systems are presented in Table IV, where the BER slopes are measured by the SNR difference (dB), denoted as $\triangle SNR$, per BER decade within the range from $BER = 10^{-1}$ to $BER = 10^{-2}$ and measured based on Fig. 4 (one can also make a similar table based

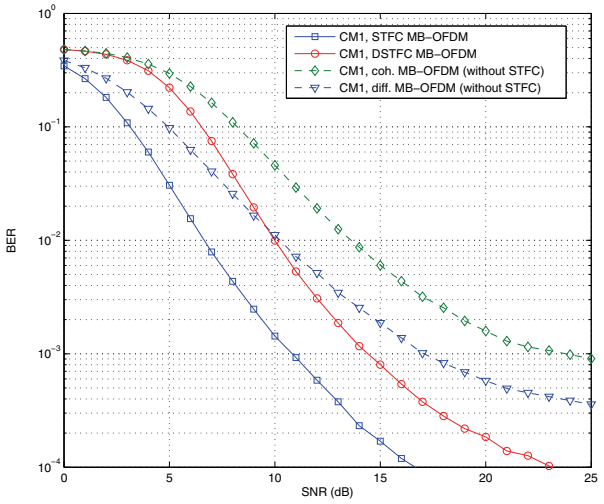

Fig. 7. Comparison between STFC MB-OFDM, DSTFC MB-OFDM, coherent MB-OFDM (without STFCs), and differential MB-OFDM (without STFCs) in CM1 with one Rx antenna.

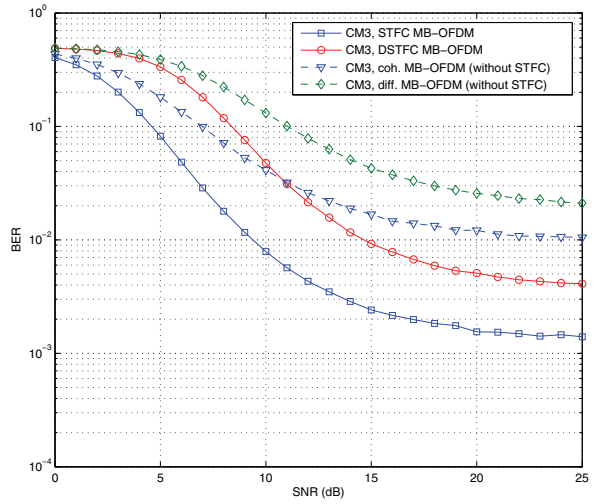

Fig. 8. Comparison between STFC MB-OFDM, DSTFC MB-OFDM, coherent MB-OFDM (without STFCs), and differential MB-OFDM (without STFCs) in CM3 with one Rx antenna.

on Fig. 3). With this slope definition, the smaller the slope is, the higher the diversity order is. From Table IV, the BER curves in the Alamouti DSFTC system are always steeper than those in the conventional differential system in all channel models CM1-CM4 respectively. It can also be seen that, when transiting from a less dispersive channel to a more dispersive one, the slopes of the BER curves in the Alamouti DSFTC system vary less than those in the conventional differential system. This means that, when the channel becomes more dispersive, the error performance degradation in the proposed DSTFC system is less sensitive to the channel dispersion, compared to the conventional differential system, though the performance degradation occurs in both systems as analyzed in Section V-C.

Figures 5 and 6 compare the bit error performance of the two Alamouti DSTFC MB-OFDM systems with QPSK (dashed curves) and DCM schemes (solid curves) with one and two Rx antennas respectively. We can realize that the proposed DSTFC MB-OFDM system associated with DCM is significantly better than the proposed DSTFC MB-OFDM system associated with QPSK, especially at high SNRs. For illustration, in CM1, the former may possess the gains of approximate 6 dB and 2.5 dB over the latter in the case of one and two Rx antennas at $BER = 10^{-4}$, respectively. Again, these gains were achieved without the increase of total transmission power, but due to the better deployment of frequency and time diversities by the DCM proposed in Section IV-B.

Fig. 7 compares all four systems, namely (coherent) STFC MB-OFDM, DSTFC MB-OFDM, conventional (coherent) MB-OFDM (without STFCs), and conventional differential MB-OFDM (without STFCs), in the channel model CM1 with one Rx antenna. Fig. 8 provides the comparison for the channel model CM3. From these figures, one can observe that the conventional differential and conventional coherent MB-OFDM systems (two dashed curves) have the same diversity orders (illustrated by the slopes of the curves), and there exists a gap of 3 dB as a penalty of missing the exact CSI at the receiver. Similarly, it is clear that the diversity orders of the STFC MB-OFDM and DSTFC MB-OFDM systems (two solid curves) are the same as pointed out in Section V-B. The advantage of 3 dB of the STFC MB-OFDM system requires the exact CSI at the receiver, i.e. requiring the transmission of a large number of MB-OFDM symbols for channel estimation, which might be uneconomical in some cases, such as the one mentioned in Example 2.

Finally, Figures 9 and 10 illustrate the effect of the different FFT/IFFT sizes to the performance of the proposed DSTFC MB-OFDM system, with the number of Tx antennas $M = 2$ (the Alamouti DSTFC is simulated) and the number of Rx antennas $N = 1$ and $N = 2$. Specifically, Fig. 9 compares the system performance between two FFT sizes, namely $N_{\text{fft}} = 64$ and $N_{\text{fft}} = 128$, in the same channel model CM1, while Fig. 10 compares the system performance in the channel model CM3. From the two figures, two important observations can be drawn. First, the larger the FFT size is, the better the system error performance is. This observation confirms the analysis stated previously in Section V-C. Second, in each figure, the two curves corresponding to the pairs ($N_{\text{fft}} = 64$, $N = 2$) and ($N_{\text{fft}} = 128$, $N = 1$) are in parallel, i.e. the two curves have the same slopes. In other words, the DSTFC MB-OFDM UWB system has the same diversity orders in these cases. This observation further verifies the mathematical analysis of diversity order, which is the product MNN_{fft} as mentioned in Section V-B.

VII. Conclusions

The paper has proposed for the first time the framework of DSTFC MB-OFDM UWB systems using the unitary Alamouti DSTFC with either constant envelope modulation scheme or multi-dimensional modulation one. The proposed DSTFC MB-OFDM concept is useful when the transmission of a large number of MB-OFDM symbols for the channel estimation

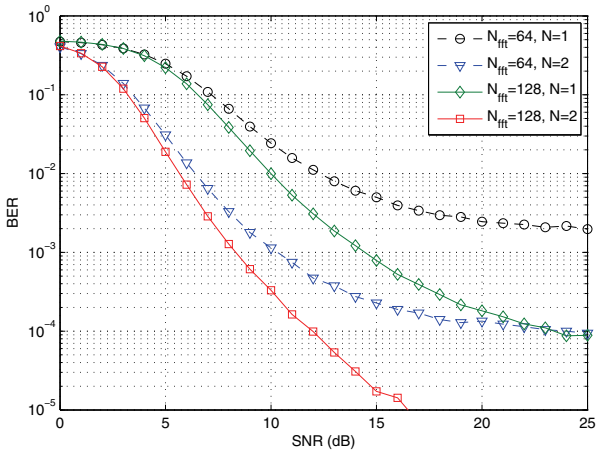

Fig. 9. Comparison between $N_{\text{fft}} = 64$ and $N_{\text{fft}} = 128$ in CM1.

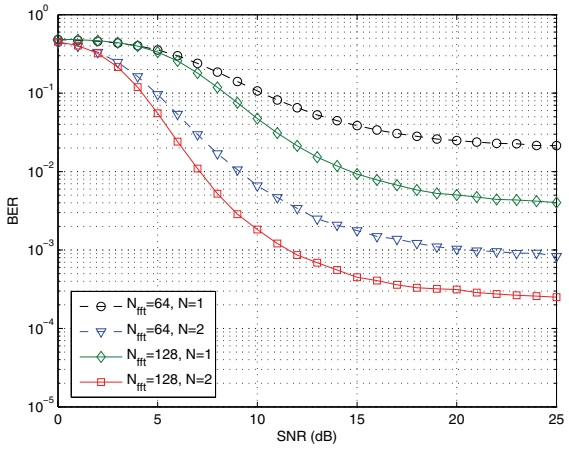

Fig. 10. Comparison between $N_{\text{fft}} = 64$ and $N_{\text{fft}} = 128$ in CM3.

purpose is uneconomical or even impractical. It has been shown that the DSTFC MB-OFDM system could provide much better bit error performance, compared to the conventional differential MB-OFDM UWB without MIMO, and even better than the conventional coherent MB-OFDM system without MIMO at a high SNR range. The improvement is achieved without any increase of total transmission power, but thanks to the spatial, temporal and frequency diversities introduced by the proposed system. The paper has also derived the novel coding and decoding algorithms for the proposed DSTFC MB-OFDM system and the in-depth analyses of the diversity order and the factors affecting the performance of a realistic MB-OFDM UWB system.

Furthermore, beside the case study of MB-OFDM UWB systems, it is our conjecture that the proposed DSTFC principle might be applied to various other wireless systems, such as WiMax MIMO [34, p.578], providing better BER than the respective WiMax without MIMO. Examination of the application of DSTFCs in WiMax MIMO might be our future work.

ACKNOWLEDGMENT

L. C. Tran would like to thank the Alexander von Humboldt (AvH) Foundation, Germany, for its support of this work in form of a postdoctoral fellowship. The authors are grateful to Prof. Vahid Tarokh, Harvard University, U.S.A for his helpful advices on the diversity order, and to anonymous reviewers for their insightful comments.

APPENDIX
PROOF OF EQUATION (20)

We need to prove that

$$\Re\{\text{tr}[\mathbb{W}_{t-1}\mathbb{H}_t\mathbb{H}_t^H\mathbb{W}_{t-1}^H\mathbb{S}_t^H\mathbb{X}_{t,m,k}]\} = \Re\{\text{tr}[(\mathbb{H}_t\mathbb{H}_t^H)(\mathbb{S}_t^H\mathbb{X}_{t,m,k})]\}. \quad (36)$$

Denote

$$\Psi = \mathbb{W}_{t-1}\mathbb{H}_t\mathbb{H}_t^H\mathbb{W}_{t-1}^H, \;\; \Omega = \mathbb{H}_t\mathbb{H}_t^H, \;\; \Xi = \mathbb{S}_t^H\mathbb{X}_{t,m,k}.$$

It is trivial to realize that Ψ and Ω are Hermitian matrices. Hence they can be presented as

$$\Psi = \begin{bmatrix} \Psi_{11} & \Psi_{12} \\ \Psi_{12}^H & \Psi_{22} \end{bmatrix}, \;\; \Omega = \begin{bmatrix} \Omega_{11} & \Omega_{12} \\ \Omega_{12}^H & \Omega_{22} \end{bmatrix},$$

where Ψ_{11}, Ψ_{12}, Ψ_{22} and Ω_{12} are all square complex diagonal matrices of size $N_{\text{fft}} \times N_{\text{fft}}$, while Ω_{11} and Ω_{22} are positive semi-definite square real diagonal matrices of size $N_{\text{fft}} \times N_{\text{fft}}$.

Recall that (cf. (9) and (10))

$$\mathbb{S}_t = 1/\sqrt{2}\begin{bmatrix} \text{diag}(\bar{\mathbf{s}}_{t,1}) & \text{diag}(\bar{\mathbf{s}}_{t,2}) \\ -\text{diag}(\bar{\mathbf{s}}_{t,2}^*) & \text{diag}(\bar{\mathbf{s}}_{t,1}^*) \end{bmatrix}, \quad (37)$$

$$\mathbb{W}_t = \mathbb{S}_t\mathbb{W}_{t-1}, \quad (38)$$

it is easy to check that the unitary matrix $\mathbb{W}_t$ constructed according to (38) (similarly for $\mathbb{W}_{t-1}$) can be presented in the following form

$$\mathbb{W}_t = \begin{bmatrix} \mathbb{W}_{11} & \mathbb{W}_{12} \\ -\mathbb{W}_{12}^H & \mathbb{W}_{11}^H \end{bmatrix},$$

where $\mathbb{W}_{11}$ and $\mathbb{W}_{12}$ are square complex diagonal matrices satisfying

$$\mathbb{W}_{11}^H\mathbb{W}_{11} = \mathbb{W}_{12}^H\mathbb{W}_{12} = \frac{1}{2}I_{N_{\text{fft}}}. \quad (39)$$

To prove (36), we first prove the following theorem.

Theorem 1: Prove that

$$\Psi_{11} + \Psi_{22} = \Omega_{11} + \Omega_{22}. \quad (40)$$

Proof: We have

$$\begin{aligned} \Psi &= \mathbb{W}_{t-1}\mathbb{H}_t\mathbb{H}_t^H\mathbb{W}_{t-1}^H, \\ &= \begin{bmatrix} \mathbb{W}_{11} & \mathbb{W}_{12} \\ -\mathbb{W}_{12}^H & \mathbb{W}_{11}^H \end{bmatrix}\begin{bmatrix} \Omega_{11} & \Omega_{12} \\ \Omega_{12}^H & \Omega_{22} \end{bmatrix}\begin{bmatrix} \mathbb{W}_{11}^H & -\mathbb{W}_{12} \\ \mathbb{W}_{12}^H & \mathbb{W}_{11} \end{bmatrix}. \end{aligned}$$

The two sub-matrices Ψ_{11} and Ψ_{22} of Ψ are calculated as

$$\begin{aligned} \Psi_{11} &= \mathbb{W}_{11}\Omega_{11}\mathbb{W}_{11}^H + \mathbb{W}_{12}\Omega_{22}\mathbb{W}_{12}^H + \\ &\quad \mathbb{W}_{11}\Omega_{12}\mathbb{W}_{12}^H + \mathbb{W}_{12}\Omega_{12}^H\mathbb{W}_{11}^H, \\ \Psi_{22} &= \mathbb{W}_{12}^H\Omega_{11}\mathbb{W}_{12} + \mathbb{W}_{11}^H\Omega_{22}\mathbb{W}_{11} - \\ &\quad \mathbb{W}_{12}^H\Omega_{12}\mathbb{W}_{11} - \mathbb{W}_{11}^H\Omega_{12}^H\mathbb{W}_{12}. \end{aligned} \quad (41)$$

$$\Psi\Xi = \begin{bmatrix} \vdots & \cdots & \ddots & \cdots & \vdots \\ \vdots & \Psi(k,k)p - \Psi(k,N_{\text{fft}}+k)q^* & \cdots & \Psi(k,k)q + \Psi(k,N_{\text{fft}}+k)p^* & \vdots \\ \vdots & \vdots & \ddots & \vdots & \vdots \\ \vdots & \Psi(N_{\text{fft}}+k,k)p - \Psi(N_{\text{fft}}+k,N_{\text{fft}}+k)q^* & \cdots & \Psi(N_{\text{fft}}+k,k)q + \Psi(N_{\text{fft}}+k,N_{\text{fft}}+k)p^* & \vdots \\ \vdots & \cdots & \ddots & \cdots & \vdots \end{bmatrix}$$

From (39) and because all matrices on the right hand side of (41) are square diagonal matrices, we can rewrite (41) as follows

$$\begin{aligned} \Psi_{11} &= \frac{1}{2}\Omega_{11} + \frac{1}{2}\Omega_{22} + \mathbb{W}_{11}\Omega_{12}\mathbb{W}_{12}^H + \mathbb{W}_{12}\Omega_{12}^H\mathbb{W}_{11}^H, \\ \Psi_{22} &= \frac{1}{2}\Omega_{11} + \frac{1}{2}\Omega_{22} - \mathbb{W}_{11}\Omega_{12}\mathbb{W}_{12}^H - \mathbb{W}_{12}\Omega_{12}^H\mathbb{W}_{11}^H. \end{aligned}$$

As a result, we have

$$\Psi_{11} + \Psi_{22} = \Omega_{11} + \Omega_{22}.$$

Eq.(40) has been proved. ■

If we denote the k-th entry ($k = 1, \ldots, N_{\text{fft}}$) of the main diagonal of Ψ (or Ω) to be $\Psi(k,k)$ ($\Omega(k,k)$), from (40), we can deduce that

$$\Psi(k,k)+\Psi(N_{\text{fft}}+k,N_{\text{fft}}+k) = \Omega(k,k)+\Omega(N_{\text{fft}}+k,N_{\text{fft}}+k). \quad (42)$$

It is also worthwhile to note that $\Psi(k,k)$, $\Psi(N_{\text{fft}}+k,N_{\text{fft}}+k)$, $\Omega(k,k)$ and $\Omega(N_{\text{fft}}+k,N_{\text{fft}}+k)$ are all real numbers since they are in the main diagonals of the Hermitian matrices Ψ and Ω.

We now return to prove Eq.(36). Recall that $\mathbb{X}_{t,m,k}$ ($m = 1,2; k = 1, \ldots, N_{\text{fft}}$) is the weighting matrix of the real part of the symbol $s_{t,m,k}$ (cf. (12)), which is in turn an element of the column vector $\bar{\mathbf{s}}_{t,m}$ in the matrix $\mathbb{S}_t$ in (37). Since $s_{t,m,k}$ only appears twice in the matrix $\mathbb{S}_t$, $\mathbb{X}_{t,m,k}$ is a real square matrix of size $2N_{\text{fft}} \times 2N_{\text{fft}}$ with all zero entries, except for two entries of $+1$ or -1. Therefore, $\Xi = \mathbb{S}_t^H\mathbb{X}_{t,m,k}$ is a square matrix of size $2N_{\text{fft}} \times 2N_{\text{fft}}$ with all zero entries, except for the four entries $\Xi(k,k)$, $\Xi(N_{\text{fft}}+k,k)$, $\Xi(k,N_{\text{fft}}+k)$, and $\Xi(N_{\text{fft}}+k,N_{\text{fft}}+k)$. Further, these four entries have the following properties

$$\begin{aligned} \Xi(k,k) &= \Xi(N_{\text{fft}}+k,N_{\text{fft}}+k)^* \\ \Xi(k,N_{\text{fft}}+k) &= -\Xi(N_{\text{fft}}+k,k)^*. \end{aligned}$$

For brevity, we denote $\Xi(k,k) = p$ and $\Xi(k,N_{\text{fft}}+k) = q$, then Ξ has the following form

$$\Xi = \begin{bmatrix} \vdots & \ddots & \cdots & \ddots & \cdots & \ddots & \vdots \\ \vdots & \cdots & p & \cdots & q & \cdots & \vdots \\ \vdots & \cdots & \vdots & \ddots & \vdots & \cdots & \vdots \\ \vdots & \cdots & -q^* & \cdots & p^* & \cdots & \vdots \\ \vdots & \ddots & \cdots & \ddots & \cdots & \ddots & \vdots \end{bmatrix},$$

where other entries of this matrix are all zeros. It is now trivial to realize that $\Psi\Xi$ contains all zeros entries, except for the (k,k), $(k,N_{\text{fft}}+k)$, $(N_{\text{fft}}+k,k)$ and $(N_{\text{fft}}+k,N_{\text{fft}}+k)$ entries (see the equation on the top of this page). As a result, we have

$$\begin{aligned} \text{tr}(\Psi\Xi) &= \Psi(k,k)p - \Psi(k,N_{\text{fft}}+k)q^* + \Psi(N_{\text{fft}}+k,k)q \\ &+ \Psi(N_{\text{fft}}+k,N_{\text{fft}}+k)p^*. \end{aligned}$$

Because $\Psi(k,k)$ and $\Psi(N_{\text{fft}}+k,N_{\text{fft}}+k)$ are real numbers and $\Psi(N_{\text{fft}}+k,k) = \Psi(k,N_{\text{fft}}+k)^*$ (Ψ is a Hermitian matrix), we may write

$$\Re\{\text{tr}(\Psi\Xi)\} = [\Psi(k,k) + \Psi(N_{\text{fft}}+k,N_{\text{fft}}+k)]\Re\{p\}. \quad (43)$$

Similarly, we can also prove that

$$\Re\{\text{tr}(\Omega\Xi)\} = [\Omega(k,k) + \Omega(N_{\text{fft}}+k,N_{\text{fft}}+k)]\Re\{p\}. \quad (44)$$

From (42), (43) and (44), it is clear that $\Re\{\text{tr}(\Psi\Xi)\} = \Re\{\text{tr}(\Omega\Xi)\}$. In other words, (36) has been proved.

REFERENCES

[1] L. C. Tran and A. Mertins, "Differential space-time-frequency codes for MB-OFDM UWB with dual carrier modulation," *Proc. 2009 IEEE Int. Conf. Commun.*, pp. 1–5.

[2] L. C. Tran, A. Mertins, E. Dutkiewicz, and X. Huang, "Unitary differential space-time-frequency codes for MB-OFDM UWB," *Proc. 2009 IEEE Int. Symp. Commun. Inform. Technol.*, pp. 1161–1166.

[3] A. Batra *et al.*, "Multiband OFDM physical layer specification," *WiMedia Alliance Release 1.1*, July 2005.

[4] W. Abbott *et al.*, "Multiband OFDM physical layer specification," *WiMedia Alliance Release 1.5*, Aug. 2009.

[5] T.-H. Tan and K.-C. Lin, "Performance of space-time block coded MB-OFDM UWB systems," *Proc. 2006 Annual Communication Networks and Services Research Conference*, pp. 323–327.

[6] W. P. Siriwongpairat, W. Su, M. Olfat, and K. J. R. Liu, "Multiband-OFDM MIMO coding framework for UWB communication systems," *IEEE Trans. Signal Process.*, vol. 54, no. 1, pp. 214–224, Jan. 2006.

[7] L. C. Tran and A. Mertins, "Space-time frequency code implementation in MB-OFDM UWB communications: design criteria and performance," *IEEE Trans. Wireless Commun.*, vol. 8, no. 2, pp. 701–713, Feb. 2009.

[8] L. C. Tran, A. Mertins, E. Dutkiewicz, and X. Huang, "Space-time-frequency codes in MB-OFDM UWB communications: advanced order-8 STFC and its performance," *Proc. 2007 IEEE International Symposium on Communications and Information Technologies*, pp. 380–385.

[9] L. C. Tran, A. Mertins, and T. A. Wysocki, "Quasi-orthogonal space-time-frequency codes in MB-OFDM UWB communications," *Proc. 2007 International Conference on Signal Processing and Communication Systems*.

[10] L. C. Tran and A. Mertins, "On the use of quasi-orthogonal space-time-frequency codes in MB-OFDM UWB," *Proc. 2008 IEEE International Conference on Communication and Electronics*, pp. 252–257.

[11] L. C. Tran and A. Mertins, "Application of quasi-orthogonal space-time-frequency codes in MB-OFDM UWB," *Proc. 2008 IEEE International Conference on Ultra-Wideband*, pp. 73–76.

[12] Q. Yang and K. S. Kwak, "Superimposed training for estimating of doubly-selective OFDM channels," *Proc. 2007 Int. Conf. Advanced Communication Technology*, vol. 3, pp. 1652–1655.

[13] K. Josiam and D. Rajan, "Bandwidth efficient channel estimation using super-imposed pilots in OFDM systems," *IEEE Trans. Wireless Commun.*, vol. 6, pp. 2234–2245, June 2007.

[14] S. Lu, G. Kang, Q. Zhu, and P. Zhang, "A orthogonal superimposed pilot for channel estimation in MIMO-OFDM systems," *Proc. 2007 IEEE Vehicular Technology Conference – Spring)*, pp. 2409–2413.
[15] H. Li, "Differential space-time-frequency modulation over frequency-selective fading channels," *IEEE Commun. Lett.*, vol. 7, no. 8, pp. 349–351, Aug. 2003.
[16] J. Wang and K. Yao, "Differential unitary space-time-frequency coding for MIMO OFDM systems," *Proc. 2002 IEEE Asilomar Conference on Signals, Systems and Computers*, vol. 2, pp. 1867–1871.
[17] Q. Ma, C. Tepedelenlioglu, and Z. Liu, "Differential spacetimefrequency coded OFDM with maximum multipath diversity," *IEEE Trans. Wireless Commun.*, vol. 4, no. 5, pp. 2232–2243, Sep. 2005.
[18] S. N. Diggavi, N. Al-Dhahir, A. Stamoulis, and A. R. Calderbank, "Differential space-time coding for frequency-selective channels," *IEEE Commun. Lett.*, vol. 6, no. 6, pp. 253–255, June 2002.
[19] T. Himsoon, W. Su, and K. J. R. Liu, "Single-block differential transmit scheme for broadband wireless mimo-ofdm systems," *IEEE Trans. Signal Process.*, vol. 54, no. 9, pp. 3305–3314, Sep. 2006.
[20] Z. Liu and G. B. Giannakis, "Block differentially encoded OFDM with maximum multipath diversity," *IEEE Trans. Wireless Commun.*, vol. 2, no. 3, pp. 420–423, May 2003.
[21] J. Foerster and Intel R&D, "Channel modelling sub-committee report final," IEEE P802.15 Working Group for Wireless Personal Area Networks (WPANs), IEEE P802.15-02/490r1-SG3a, Oct. 2005.
[22] S. M. Alamouti, "A simple transmit diversity technique for wireless communications," *IEEE J. Sel. Areas Commun.*, vol. 16, no. 8, pp. 1451–1458, Oct. 1998.
[23] L. C. Tran, T. A. Wysocki, A. Mertins, and J. Seberry, *Complex Orthogonal Space-Time Processing in Wireless Communications*. Springer, 2006.
[24] V. Tarokh, H. Jafarkhani, and A. R. Calderbank, "Space-time blocks codes from orthogonal designs," *IEEE Trans. Inf. Theory*, vol. 45, no. 5, pp. 1456–1467, July 1999.
[25] H. Jafarkhani, "A quasi-orthogonal space-time block codes," *IEEE Trans. Commun.*, vol. 49, no. 1, pp. 1–4, Jan. 2001.
[26] A. Batra, J. Balakrishnan, A. Dabak, *et al.*, "Multi-band OFDM physical layer proposal for IEEE 802.15 task group 3a," IEEE P802.15-04/0493r1, Sep. 2004.
[27] T. S. Rappaport, *Wireless Communication: Principles and Practice*, 2nd edition. Prentice Hall PTR, 2002.
[28] SKF Magnetic Bearings, "FQA." Available: http://www.skf.com/portal/skf_rev/home/technology?contentId=079612&lang=en#Label1 (accessed Date 17 Mar 2012).
[29] B. L. Hughes, "Differential space-time modulation," *IEEE Trans. Inf. Theory*, vol. 46, no. 7, pp. 2567–2578, Nov. 2000.
[30] L. Zheng and D. N. C. Tse, "Diversity and multiplexing: a fundamental tradeoff in multiple-antenna channels," *IEEE Trans. Inf. Theory*, vol. 49, no. 5, pp. 1073–1096, May 2003.
[31] V. Tarokh and H. Jafarkhani, "A differential detection scheme for transmit diversity," *IEEE J. Sel. Areas Commun.*, vol. 18, no. 7, pp. 1169–1174, July 2000.
[32] J. C-I Chuang, "Comparison of coherent and differential detection of BPSK and QPSK in a quasi-static fading channel," in *Proc. 1988 IEEE Int. Conf. Commun.*, vol. 2, pp. 749–755.
[33] G. Ganesan and P. Stoica, "Differential modulation using space-time block codes," *IEEE Signal Process. Lett.*, vol. 9, no. 2, pp. 57–60, Feb. 2002.
[34] R. B. Marks *et al.*, "IEEE standard for local and metropolitan area networks. Part 16: Air interface for fixed and mobile broadband wireless access systems. Amendment 2: Physical and medium access control layers for combined fixed and mobile operation in licensed bands and corrigendum 1," IEEE 802.16e-2005, Feb. 2006.

Le Chung Tran (MIEEE, Humboldtian) received the excellent B. Eng. degree (highest distinction), M. Eng. (highest distinction), and PhD in telecommunications engineering, from Hanoi University of Communications and Transport (UCT), Hanoi University of Technology (HUT), Vietnam, and the University of Wollongong (UOW), Australia, in 1997, 2000, and 2006, respectively. He was with UCT as a lecturer from 1997 to 2002. From 2002 to 2005, he was a part-time teaching academic, and from 2005 to 2006, he was an Associate Research Fellow at UOW, Australia. He was then a Research Fellow in Germany under the postdoctoral research fellowship from the Alexander von Humboldt (AvH) foundation from 2006 to 2008. In 2009, he joined the University of Wollongong, Australia, as a lecturer. He has achieved a number of national and overseas awards, including WUS – World University Services (twice), Vietnamese government's scholarship, UPA – Wollongong University Postgraduate Award, Wollongong university tuition fee waiver, and the AvH postdoctoral research fellowship. He has published one book, one book chapter, and over 35 research papers. He has served as a TPC member, session chair/co-chair and/or publicity chair for 15 IEEE conferences. His research interests include MIMO, space-time-frequency processing, UWB, mobile communications, wireless communications, DSP for communications, network coding and software defined radio.

Alfred Mertins (SMIEEE) received his Dipl.-Ing. degree from the University of Paderborn, Germany, in 1984, the Dr.-Ing. degree in Electrical Engineering and the Dr.-Ing. habil. degree in Telecommunications from the Hamburg University of Technology, Germany, in 1991 and 1994, respectively. From 1986 to 1991 he was a Research Assistant at the Hamburg University of Technology, Germany, and from 1991 to 1995 he was a Senior Scientist at the Microelectronics Applications Center Hamburg, Germany. From 1996 to 1997 he was with the University of Kiel, Germany, and from 1997 to 1998 with the University of Western Australia. In 1998, he joined the University of Wollongong, where he was at last an Associate Professor of Electrical Engineering. From 2003 to 2006, he was a Professor in the Faculty of Mathematics and Science at the University of Oldenburg, Germany. In November 2006, he joined the University of Lübeck, Germany, where he is a Professor and Director of the Institute for Signal Processing. He has written two books and published over 100 research papers. His research interests include speech, audio, and image processing, wavelets and filter banks, pattern recognition, and digital communications.

Tadeusz A. Wysocki (SMIEEE) received the M.Sc.Eng. degree with the highest distinction in telecommunications from the Academy of Technology and Agriculture, Bydgoszcz, Poland, in 1981. In 1984, he received his Ph.D. degree, and in 1990, was awarded a D.Sc. degree (habilitation) in telecommunications from the Warsaw University of Technology. In 1992, Dr. Wysocki moved to Perth, Western Australia to work at Edith Cowan University. He spent the whole 1993 at the University of Hagen, Germany, within the framework of Alexander von Humboldt Research Fellowship. After returning to Australia, he was appointed a Program Leader, Wireless Systems, within Cooperative Research Centre for Broadband Telecommunications and Networking. From 1998 to 2007 he was an Associate Professor at the University of Wollongong, NSW, within the School of Electrical, Computer and Telecommunications Engineering, and in 2007 he joined the University of Nebraska-Lincoln as a Professor of Computer and Electronics Engineering. The main areas of Dr. Wysocki's research interests include: indoor propagation of microwaves, digital modulation and coding schemes as well as biological communications at nano-scale. He is the author or co-author of four books, over 250 research publications and nine patents.